# Millimeter-Wave Beamformed Full-dimensional MIMO Channel Estimation Based on Atomic Norm Minimization

Yingming Tsai, *Member, IEEE,* Le Zheng, *Member, IEEE,*

and Xiaodong Wang, *Fellow, IEEE*

Electrical Engineering Dept., Columbia Univ., New York, NY 10027

## Abstract

The millimeter-wave (mmWave) full-dimensional (FD) MIMO system employs planar arrays at both the base station and user equipment and can simultaneously support both azimuth and elevation beamforming. In this paper, we propose atomic-norm-based methods for mmWave FD-MIMO channel estimation under both uniform planar arrays (UPA) and non-uniform planar arrays (NUPA). Unlike existing algorithms such as compressive sensing (CS) or subspace methods, the atomic-norm-based algorithms do not require to discretize the angle spaces of the angle of arrival (AoA) and angle of departure (AoD) into grids, thus provide much better accuracy in estimation. In the UPA case, to reduce the computational complexity, the original large-scale 4D atomic norm minimization problem is approximately reformulated as a semi-definite program (SDP) containing two decoupled two-level Toeplitz matrices. The SDP is then solved via the alternating direction method of multipliers (ADMM) where each iteration involves only closed-form computations. In the NUPA case, the atomic-norm-based formulation for channel estimation becomes nonconvex and a gradient-decent-based algorithm is proposed to solve the problem. Simulation results show that the proposed algorithms achieve better performance than the CS-based and subspace-based algorithms.

**Keywords:** Full-dimensional (FD) MIMO, uniform planar array (UPA), non-uniform planar array (NUPA), atomic norm, channel estimation, millimeter-wave, alternating direction method of multipliers (ADMM), gradient descent.

# I. INTRODUCTION

Millimeter wave (mmWave) communications have been proposed as an important physical-layer technology for the 5th generation (5G) mobile networks to provide multi-gigabit services [1]. Two prominent features of the mmWave spectrum are the massive bandwidth available and the tiny wavelengths compared to conventional microwave bands, thus enabling dozens or even hundreds of antenna elements to be accommodated at communication link ends within a reasonable physical form factor. This suggests that massive MIMO and mmWave technologies should be considered jointly to provide higher data rates and spectrum efficiency. In particular, the mmWave full-dimensional MIMO (FD-MIMO) systems [2],[3] employ uniform or non-uniform planar arrays at both the basestation (BS) and user equipment (UE) and provide an extra degree of freedom in the elevation-angle domain. Users can now be distinguished not only by their AoAs in the azimuth domain but also by their AoDs in the elevation domain [4]. In this paper, we consider channel estimation for mmWave FD-MIMO systems that simultaneously support both azimuth and elevation beamforming.

The mmWave band channel is significantly different from those in sub-6GHz bands. The key challenge in designing new radio access technologies for mmWave is how to overcome the much larger path-loss and reduce blockage probability. To that end, beamforming is essential in combating the serve path-loss for wireless system operating in mmWave bands [5]. However, to estimate the full channel state information (CSI) under beamformed FD-MIMO is somehow challenging because the receiver typically only obtains the beamformed CSI instead of full CSI. To address this issue, fast beam scanning and searching techniques have been extensively studied [3], [6]. The objective of beam scanning is to search for the best beamformer-combiner pair by letting the transmitter and receiver scan the adaptive sounding beams chosen from pre-determined sounding beam codebooks. However, the exhaustive search may be hampered by the high training overhead in practice and suffer from low spectral efficiency. Another approach is to estimate the mmWave channel or its associated parameters, by exploiting the sparse scattering nature of the mmWave channels [7],[8],[9], that is, mmWave channel estimation can be formulated as a sparse signal recovery problem [10], [11], [12], [13] and solved using the compressive sensing (CS)-based approach [14]. In the CS-based approach, a sensing matrix needs to be constructed first, by dividing certain parameter space into a

finite number of grids and thus the channel estimation performance is limited by the grid resolution. On the other hand, in [15], a subspace-based mmWave MIMO channel estimation method that makes use of the MUSIC algorithm is proposed. A 2D-MUSIC algorithm for beamformed mmWave MIMO channel estimation is proposed in [12] to further enhance the channel estimation performance. The MUSIC algorithm is able to identify multiple paths with high resolution but it is sensitive to antenna position, gain, and phase errors.

Recently, the atomic norm minimization [16] has been applied to many signal processing problems such as super-resolution frequency estimation [17], [18], spectral estimation [19], AoA estimation, [20], [21], uplink multiuser MIMO channel estimation [22] and linear system identification [23]. Under certain conditions, atomic norm minimization can achieve exact frequency localization, avoiding the effects of basis mismatch which can plague grid-based CS techniques. Different from the prior works such as CS-based and subspace-based channel estimation methods mentioned above, we formulate the mmWave FD-MIMO channel estimation as an atomic norm minimization problem. Unlike [22] that considers uplink multiuser MIMO channel estimation, in which the uniform linear array is assumed and only the AoA parameter is estimated, in this paper, we consider the mmWave beamformed FD-MIMO channel, which involves the estimation of both AoA and AoD. Hence, instead of one-dimensional (1D) atomic norm minimization, our problem is formulated as a four-dimensional (4D) atomic norm minimization problem. The 4D atomic norm minimization can be transformed into semi-definite program (SDP) which is of high dimensional and involves block Toeplitz matrices, leading to very high computational complexity. Therefore, we introduce a 4D atomic norm approximation method to reduce the computational complexity and an efficient algorithm based on the alternating direction method of multipliers (ADMM) is derived.

Recently, non-uniform planar array (NUPA) has attracted more interest due to its ability in reducing sidelobes and antenna correlation [24], [25]. NUPA can potentially increase the achievable multiplexing gain of mmWave FD-MIMO beamforming. However, the corresponding atomic norm minization problem cannot be transformed into an SDP when the antennas are not uniformly placed [16]. Hence, we propose a gradient descent method for mmWave FD-MIMO channel estimation with NUPA.

The remainder of the paper is organized as follows. In Section II, the mmWave beamformed FD-MIMO channel model is introduced. In Section III, we formulate the mmWave FD-MIMO channel estimation as an atomic norm minimization problem for the case of UPA. In Section IV, we develop efficient algorithms for implementing the proposed atomic-norm-based channel estimator. In Section V, we consider the case of NUPA and provide the formulation and algorithm for the atomic-norm-based channel estimator. In Section VI, simulation results are provided. Finally, Section VII concludes the paper.

## II. SYSTEM DESCRIPTIONS AND BACKGROUND

### A. System and Channel Models

We consider a mmWave FD-MIMO system with $M$ receive antennas and $N$ transmit antennas that simultaneously supports elevation and azimuth beamforming. The channel matrix can be expressed in terms of transmit and receive array responses [9]:

$$\mathbf{H} = \mathbf{B}\boldsymbol{\Sigma}\mathbf{A}^H = \sum_{l=1}^{L} \sigma_l \mathbf{b}(\mathbf{f}_l)\mathbf{a}(\mathbf{g}_l)^H, \tag{1}$$

where $(\cdot)^H$ denotes the Hermitian transpose; the matrix $\boldsymbol{\Sigma} = \mathrm{diag}(\boldsymbol{\sigma}) = \mathrm{diag}\left([\sigma_1 \; \sigma_2 \ldots \sigma_L]^T\right)$ is a diagonal matrix with each $\sigma_l \in \mathbb{C}$ denoting the $l$-th multipath gain; $L$ denotes the number of paths; the matrices $\mathbf{B} = [\mathbf{b}(\mathbf{f}_1)\ldots\mathbf{b}(\mathbf{f}_L)]$ and $\mathbf{A} = [\mathbf{a}(\mathbf{g}_1)\ldots\mathbf{a}(\mathbf{g}_L)]$ denote the steering responses of the receive and transmit arrays, respectively. For a linear array with half-wavelength separation of adjacent antenna elements, the array response is in the form of a uniformly sampled complex sinusoid with frequency $x \in [-\frac{1}{2}, \; \frac{1}{2})$:

$$\mathbf{c}_n(x) = \frac{1}{\sqrt{n}}\left[1 \; e^{j2\pi x} \cdots e^{j2\pi(n-1)x}\right]^T \in \mathbb{C}^{n \times 1}. \tag{2}$$

We assume that both the transmitter (Tx) and receiver (Rx) are equipped with uniformly spaced planar antenna arrays (UPA)s [26], [27], each with half-wavelength antenna element separations along the elevation-and-azimuth-axis. Then the Tx and Rx array responses can be expressed as [27]

$$\mathbf{a}(\mathbf{g}_l) = \mathbf{c}_{N_1}(g_{l,1}) \otimes \mathbf{c}_{N_2}(g_{l,2}), \tag{3}$$

$$\mathbf{b}(\mathbf{f}_l) = \mathbf{c}_{M_1}(f_{l,1}) \otimes \mathbf{c}_{M_2}(f_{l,2}), \tag{4}$$

with

$$\mathbf{g}_l \;=\; \left\{ g_{l,1} = \frac{1}{2}\sin\left(\vartheta_l\right)\cos\left(\varphi_l\right), g_{l,2} = \frac{1}{2}\cos\left(\vartheta_l\right) \right\}, \tag{5}$$

$$\mathbf{f}_l \;=\; \left\{ f_{l,1} = \frac{1}{2}\sin\left(\theta_l\right)\cos\left(\phi_l\right), f_{l,2} = \frac{1}{2}\cos\left(\theta_l\right) \right\}, \tag{6}$$

where $\otimes$ denotes the Kronecker product; $\vartheta_l$, $\varphi_l$ denote elevation and azimuth angles of the angle of departure (AoD) of the $l$-th path, respectively; and $\theta_l$, $\phi_l$ denote elevation and azimuth angles of the angle of arrival (AoA), respectively. Here, $N_1$, $N_2$ denote the numbers of elevation and azimuth transmit antennas, respectively, and the total number of transmit antennas is $N = N_1 N_2$. Similarly, $M_1$, $M_2$ denote the numbers of elevation and azimuth receive antennas, respectively, and the total number of receive antennas is $M = M_1 M_2$. For the UPA configuration, it can resolve the AoA and AoD in $360°$ range, thereby $\vartheta_l, \theta_l, \varphi_l, \phi_l \in [-\pi, \ \pi]$ and $g_{l,1} = \frac{1}{2}\sin\left(\vartheta_l\right)\cos\left(\varphi_l\right) \in [-\frac{1}{2}, \ \frac{1}{2})$, $g_{l,2} = \frac{1}{2}\cos\left(\vartheta_l\right) \in [-\frac{1}{2}, \ \frac{1}{2})$, $f_{l,1} = \frac{1}{2}\sin\left(\theta_l\right)\cos\left(\phi_l\right) \in [-\frac{1}{2}, \frac{1}{2})$, $f_{l,2} = \frac{1}{2}\cos\left(\theta_l\right) \in [-\frac{1}{2}, \frac{1}{2})$.

To estimate the channel matrix, the transmitter transmits $P$ distinct beams during $P$ successive time slots. i.e., in the $p$-th time slot, the beamforming vector $\mathbf{p}_p \in \mathbb{C}^{N \times 1}$ is selected from a set of unitary vectors in the form of Kronecker-product-based codebook, e.g., $\mathbf{p}_p = \mathbf{p}_{p,1} \otimes \mathbf{p}_{p,2}$ where $\mathbf{p}_{p,1} \in \mathbb{C}^{N_1}$ and $\mathbf{p}_{p,2} \in \mathbb{C}^{N_2}$ are selected from two DFT codebooks of dimensions $N_1$ and $N_2$, respectively [28]. The $p$-th received signal vector can be expressed as

$$\mathbf{y}_p = \mathbf{H}\mathbf{p}_p s_p + \mathbf{w}_p, \tag{7}$$

where $\mathbf{w}_p \sim \mathcal{CN}\left(\mathbf{0}, \sigma_w^2 \mathbf{I}_M\right)$ is the additive white Gaussian noise (AWGN) with $\mathbf{I}_M$ denoting the $M \times M$ identity matrix, and $s_p$ denotes the pilot symbol in the $p$-th time slot. The receiver collects $\mathbf{y}_p \in \mathbb{C}^{M \times 1}$ for $p = 1, \ldots P$ and concatenates them to obtain the signal matrix

$$\mathbf{Y} = [\mathbf{y}_1 \ \mathbf{y}_2 \ldots \mathbf{y}_P] = \mathbf{H}\mathbf{P}\mathbf{S} + \mathbf{W} = \mathbf{B}\mathbf{\Sigma}\mathbf{A}^H \mathbf{P}\mathbf{S} + \mathbf{W}, \tag{8}$$

where $\mathbf{P} = [\mathbf{p}_1 \ \mathbf{p}_2 \ldots \mathbf{p}_P] \in \mathbb{C}^{N \times P}$, $\mathbf{W} = [\mathbf{w}_1 \ \mathbf{w}_2 \ldots \mathbf{w}_P] \in \mathbb{C}^{M \times P}$ and $\mathbf{S} = \mathrm{diag}\left([s_1 \ s_2 \ldots s_P]\right) \in \mathbb{C}^{P \times P}$. For simplicity, we assume that $\mathbf{S} = \sqrt{P_t}\mathbf{I}_P$, where $P_t$ is the power of the pilot symbol. Then we have

$$\mathbf{Y} = \sqrt{P_t}\mathbf{H}\mathbf{P} + \mathbf{W} = \sqrt{P_t}\mathbf{B}\mathbf{\Sigma}\mathbf{A}^H \mathbf{P} + \mathbf{W}. \tag{9}$$

Our goal is to estimate the channel matrix $\mathbf{H} \in \mathbb{C}^{M \times N}$ from the measurements $\mathbf{Y} \in \mathbb{C}^{M \times P}$. Note that the number of pilots is usually smaller than the number of transmit antennas, i.e., $P < N$. Hence, we need to exploit the sparsity of $\mathbf{H}$ for its estimation, which will be discussed in the next section.

### B. Existing mmWave Channel Estimation Methods

Before describing our proposed mmWave channel estimator, we briefly discuss some existing mmWave channel estimation methods [10], [29], [13], [12] which can be divided into two categories.

*1) CS-based mmWave channel estimators:* The mmWave channel is usually composed of small number of propagation paths and CS-based algorithms have been developed [10], [29], [13] for channel estimation. First the dictionary matrices $\mathbf{A}_D \in \mathbb{C}^{N \times N_G}$ and $\mathbf{B}_D \in \mathbb{C}^{M \times N_G}$ are constructed based on quantized AoD angle of the transmitter and AoA angle of the receiver. The AoDs and AoAs are assumed to be taken from a uniform grid of $N_G$ points with $N_G \gg L$. The resulting dictionary matrix is expressed (take the transmitter $\mathbf{A}_D$ for example, the receiver dictionary matrix $\mathbf{B}_D$ is similar.)

$$\mathbf{A}_D = [\mathbf{a}(\bar{\mathbf{g}}_1) \ \mathbf{a}(\bar{\mathbf{g}}_2) \ldots \mathbf{a}(\bar{\mathbf{g}}_{N_G})], \tag{10}$$

where $\bar{\mathbf{g}}_i = \{\bar{g}_{i,1}, \bar{g}_{i,2}\} = \left\{\frac{1}{2} \sin(\bar{\vartheta}_i) \cos(\bar{\varphi}_i), \frac{1}{2} \cos(\bar{\vartheta}_i)\right\}$ with $\bar{\vartheta}_i = \frac{(i-1)2\pi}{N_G} - \pi$, $\bar{\varphi}_i = \frac{(i-1)2\pi}{N_G} - \pi$ denotes the transmit array response vector for the grid point $\bar{\vartheta}_i$ and $\bar{\varphi}_i$ for $i = 1, 2, \ldots, N_G$. The size $N_G$ of the angle grids can be set according to the desired angular resolution. On this basis, the received signal $\mathbf{Y}$ in (9) can be vectorized as [10]

$$\mathbf{y} = \text{vec}(\mathbf{Y}) = \sqrt{P_t} \left(\mathbf{P}^T \otimes \mathbf{I}_M\right) \text{vec}(\mathbf{H}) + \mathbf{w} \tag{11}$$

$$= \sqrt{P_t} \left(\mathbf{P}^T \otimes \mathbf{I}_M\right) (\mathbf{A}_D^* \odot \mathbf{B}_D) \mathbf{x} + \mathbf{w} = \sqrt{P_t} \mathbf{G} \mathbf{x} + \mathbf{w}, \tag{12}$$

where $\odot$ denotes the matrix Khatri-Rao products, $(\cdot)^T$ denotes the transpose operation, $(\cdot)^*$ denotes the complex conjugate, $\mathbf{x} \in \mathbb{C}^{N_G^4}$ is a sparse vector that has non-zero elements in the locations associated with the dominant paths. Note that the angle spaces of interest are discretized into a large number of grids, and the actual AoA and AoD angles may not exactly reside on the predefined grids. Those off-grid angles can lead to mismatches in the channel model and degrade the estimation performance.

*2) Subspace-based mmWave channel estimators:* Another existing approach to mmWave channel estimation is based on the subspace methods such as the MUSIC algorithm [12]. The MUSIC algorithm firstly calculates the covariance matrix of the received signal $\mathbf{Y}$ and then finds the signal and noise subspaces via eigendecomposition. It then estimates each channel path's array response, i.e., $\hat{\mathbf{g}}_l$ and $\hat{\mathbf{f}}_l$ for $l = 1, 2, \ldots, \hat{L}$, where $\hat{L}$ is the estimated number of paths, by exploiting the orthogonality between the signal and noise subspaces. Finally, each channel path's coefficient, i.e., $\hat{\sigma}_l$ can be estimated via the least-squares (LS) method. The MUSIC algorithm has been popular for its good resolution and accuracy in AoD/AoA estimation [30], [31]. However, it is also reported that the off-grid CS method [16] can outperform the MUSIC algorithm in terms of estimation accuracy in noisy environments [19], [32].

## III. CHANNEL ESTIMATION VIA ATOMIC NORM MINIMIZATION

As explained in the previous section, the performance of the mmWave channel estimators based on on-grid methods such as CS can be degraded due to grid mismatch. In this section, we propose a new mmWave channel estimator based on an off-grid CS method, i.e., the atomic norm minimization method.

### A. Background on Multi-dimensional Atomic Norm

First we briefly introduce the concept of multi-dimensional atomic norm [33]. A $d$-dimensional ($d$-dim) atom is defined as

$$\mathbf{q}_d (x_1, \ldots, x_d) = \mathbf{c}_{n_1} (x_1) \otimes \ldots \otimes \mathbf{c}_{n_d} (x_d), \tag{13}$$

where $n_i$ is the length of the normalized vector $\mathbf{c}_{n_i} (x_i)$ defined in (2) and $x_i \in \left[ -\frac{1}{2}, \frac{1}{2} \right)$ for $i = 1, 2, \ldots, d$. The $d$-dim atomic set is then given by

$$\mathcal{A} = \left\{ \mathbf{q}_d (x_1, \ldots, x_d) : x_i \in \left[ -\frac{1}{2}, \frac{1}{2} \right), \ i = 1, \ldots, d \right\}. \tag{14}$$

For any vector $\mathbf{t}_d$ of the form $\mathbf{t}_d = \sum_l \alpha_l \mathbf{q}_d(x_{l,1}, x_{l,2}, \ldots, x_{l,d})$, its $d$-dim atomic norm with respect to $\mathcal{A}$ is defined as

$$
\begin{aligned}
\|\mathbf{t}_d\|_{\mathcal{A}} &= \inf\left\{t : \mathbf{t}_d \in t\text{conv}\,(\mathcal{A})\right\}, \\
&= \inf_{\substack{x_{l,1},x_{l,2},\ldots,x_{l,d}\in[-\frac{1}{2},\frac{1}{2}) \\ \alpha_l\in\mathbb{C}}} \left\{\sum_l |\alpha_l| \,\middle|\, \mathbf{t}_d = \sum_l \alpha_l \mathbf{q}_d(x_{l,1}, x_{l,2}, \ldots, x_{l,d})\right\},
\end{aligned}
\tag{15}
$$

where conv $(\mathcal{A})$ is the convex hull of $\mathcal{A}$. The $d$-dim atomic norm of $\mathbf{t}_d$ has following equivalent form [33]:

$$
\|\mathbf{t}_d\|_{\mathcal{A}} = \inf_{\mathcal{U}_d\in\mathbb{C}^{(2n_d-1)\times(2n_{d-1}-1)\times\ldots\times(2n_1-1)},t\in\mathbb{R}} \left\{
\begin{array}{l}
\frac{1}{2n_1 n_2 \ldots n_d}\text{Tr}\,(\mathbb{T}_d(\mathcal{U}_d)) + \frac{1}{2}t \\[2ex]
\text{s.t.} \begin{bmatrix} \mathbb{T}_d(\mathcal{U}_d) & \mathbf{t}_d \\ \mathbf{t}_d^H & t \end{bmatrix} \succeq 0
\end{array}
\right\},
\tag{16}
$$

where $\text{Tr}\,(\cdot)$ is the trace of the input matrix, $\mathcal{U}_d \in \mathbb{C}^{(2n_d-1)\times(2n_{d-1}-1)\times\ldots\times(2n_1-1)}$ is a $d$-way tensor and $\mathbb{T}_d(\mathcal{U}_d)$ is a $d$-level block Toeplitz, which is defined recursively as follows. Denote $\mathbf{n}_d = (n_d, n_{d-1}, \ldots, n_1)$ and $\mathcal{U}_{d-1}(i) = \mathcal{U}_d(i, :, :, \ldots, :)$ for $i = -n_d + 1, -n_d + 2, \ldots, n_d - 1$. For $d = 1$, $\mathbf{n}_1 = (n_1)$ and $\mathbb{T}_1(\mathbf{u}_1) = \text{Toep}(\mathbf{u}_1)$ with $\mathbf{u}_1 \in \mathbb{C}^{(2n_1-1)\times 1}$, i.e.,

$$
\mathbb{T}_1(\mathbf{u}_1) = \text{Toep}(\mathbf{u}_1) = \begin{bmatrix}
u_1(0) & u_1(1) & \cdots & u_1(n_1 - 1) \\
u_1(-1) & u_1(0) & \cdots & u_1(n_1 - 2) \\
\vdots & \vdots & \ddots & \vdots \\
u_1(1 - n_1) & u_1(2 - n_1) & \cdots & u_1(0)
\end{bmatrix}.
\tag{17}
$$

For $d \geq 2$, we have

$$
\mathbb{T}_d(\mathcal{U}_d) = \begin{bmatrix}
\mathbb{T}_{d-1}(\mathcal{U}_{d-1}(0)) & \mathbb{T}_{d-1}(\mathcal{U}_{d-1}(1)) & \ldots & \mathbb{T}_{d-1}(\mathcal{U}_{d-1}(n_d - 1)) \\
\mathbb{T}_{d-1}(\mathcal{U}_{d-1}(-1)) & \mathbb{T}_{d-1}(\mathcal{U}_{d-1}(0)) & \ldots & \mathbb{T}_{d-1}(\mathcal{U}_{d-1}(n_d - 2)) \\
\vdots & \vdots & \ddots & \vdots \\
\mathbb{T}_{d-1}(\mathcal{U}_{d-1}(1 - n_d)) & \mathbb{T}_{d-1}(\mathcal{U}_{d-1}(2 - n_d)) & \ldots & \mathbb{T}_{d-1}(\mathcal{U}_{d-1}(0))
\end{bmatrix}.
\tag{18}
$$

## B. Atomic Norm Minimization Formulation

In this subsection, we formulate the atomic norm minimization problem for channel estimation. First, we vectorize the mmWave FD-MIMO channel matrix $\mathbf{H}$ in (1) as

$$
\begin{aligned}
\mathbf{h} &= \mathrm{vec}(\mathbf{H}) = \sum_{l=1}^{L} \sigma_l \mathbf{a}(\mathbf{g}_l)^* \otimes \mathbf{b}(\mathbf{f}_l) \\
&= \sum_{l=1}^{L} \sigma_l \left( \mathbf{c}_{N_1}(g_{l,1}) \otimes \mathbf{c}_{N_2}(g_{l,2}) \right)^* \otimes \left( \mathbf{c}_{M_1}(f_{l,1}) \otimes \mathbf{c}_{M_2}(f_{l,2}) \right) \\
&= \sum_{l=1}^{L} \sigma_l \mathbf{c}_{N_1}^*(g_{l,1}) \otimes \mathbf{c}_{N_2}^*(g_{l,2}) \otimes \mathbf{c}_{M_1}(f_{l,1}) \otimes \mathbf{c}_{M_2}(f_{l,2}).
\end{aligned}
\tag{19}
$$

Comparing (15) and (19), for the mmWave FD-MIMO channel with UPA configuration, the atom has the form of

$$
\mathbf{q}_4\left(\mathbf{g}, \mathbf{f}\right) = \mathbf{c}_{N_1}^*(g_1) \otimes \mathbf{c}_{N_2}^*(g_2) \otimes \mathbf{c}_{M_1}(f_1) \otimes \mathbf{c}_{M_2}(f_2),
\tag{20}
$$

and the set of atoms is defined as the collection of all normalized 4D complex sinusoids: $\mathcal{A} = \left\{ \mathbf{q}_4\left(\mathbf{g}, \mathbf{f}\right) : \mathbf{f} \in [-\frac{1}{2}, \frac{1}{2}) \times [-\frac{1}{2}, \frac{1}{2}),\ \mathbf{g} \in [-\frac{1}{2}, \frac{1}{2}) \times [-\frac{1}{2}, \frac{1}{2}) \right\}$ [34], [35]. The 4D atomic norm for any $\mathbf{h}$ defined in (19) can be written as [34]:

$$
\|\mathbf{h}\|_{\mathcal{A}} = \inf_{\substack{\mathbf{f}_l \in [-\frac{1}{2}, \frac{1}{2}) \times [-\frac{1}{2}, \frac{1}{2}), \\ \mathbf{g}_l \in [-\frac{1}{2}, \frac{1}{2}) \times [-\frac{1}{2}, \frac{1}{2}), \\ \sigma_l \in \mathbb{C}}} \left\{ \sum_l |\sigma_l| \,\middle|\, \mathbf{h} = \sum_l \sigma_l \mathbf{q}_4\left(\mathbf{g}_l, \mathbf{f}_l\right) \right\}.
\tag{21}
$$

The atomic norm can enforce sparsity in the atom set $\mathcal{A}$. On this basis, an optimization problem will be formulated for the estimation of the path frequencies $\{\mathbf{f}_l, \mathbf{g}_l\}$. For the convenience of calculation, we will use the equivalent form of the atomic norm given by (16), i.e.,

$$
\|\mathbf{h}\|_{\mathcal{A}} = \inf_{\substack{\mathcal{U}_4 \in \mathbb{C}^{(2N_1-1) \times (2N_2-1) \times (2M_1-1) \times (2M_2-1)}, \\ t \in \mathbb{R}}} \left\{ \begin{array}{l} \frac{1}{2MN} \mathrm{Tr}\left(\mathbb{T}_4(\mathcal{U}_4)\right) + \frac{1}{2}t \\[2mm] \text{s.t.} \begin{bmatrix} \mathbb{T}_4(\mathcal{U}_4) & \mathbf{h} \\ \mathbf{h}^H & t \end{bmatrix} \succeq 0 \end{array} \right\},
\tag{22}
$$

where $\mathbb{T}_4(\mathcal{U}_4)$ is a 4-level Toeplitz matrix defined in (18). Define the minimum frequency separations as

$$
\Delta_{\min, f_i} = \min_{l \neq l'} \min\{|f_{l,i} - f_{l',i}|, 1 - |f_{l,i} - f_{l',i}|\},
\tag{23}
$$

$$
\Delta_{\min, g_i} = \min_{l \neq l'} \min\{|g_{l,i} - g_{l',i}|, 1 - |g_{l,i} - g_{l',i}|\},
\tag{24}
$$

for $i = 1, 2$. To show the connection between the atomic norm and the channel matrix, we obtain the following theorem via extending Theorem 1.2 in [36] for 1D atomic norm to 4D atomic norm.

**Theorem 1.** *If the path component frequencies are sufficiently separated, i.e.,*

$$\Delta_{\min, f_i} \geq \frac{1}{\lfloor (M_i - 1)/4 \rfloor}, \tag{25}$$

$$\Delta_{\min, g_i} \geq \frac{1}{\lfloor (N_i - 1)/4 \rfloor}, \tag{26}$$

*for $i = 1, 2$, then we have $\|\mathbf{h}\|_{\mathcal{A}} = \sum_l |\sigma_l|$, so the component atoms of $\mathbf{h}$ can be uniquely located via computing its atomic norm.*

The proof follows the same line as that in Theorem 1.2 [36], with the dual polynomial constructed by interpolation with a 4D kernel. The theorem holds because all bounds in the proof of [Theorem 1.2, 34] hold by leveraging the 1D results.

To estimate the mmWave FD-MIMO channel $\mathbf{H}$ in (1) based on the signal $\mathbf{Y}$ in (9), we then formulate the following optimization problem:

$$\hat{\mathbf{h}} = \min_{\mathbf{h} \in \mathbb{C}^{MN}} \mu \|\mathbf{h}\|_{\mathcal{A}} + \frac{1}{2} \left\| \mathbf{y} - \sqrt{P_t} \left( \mathbf{P}^T \otimes \mathbf{I}_M \right) \mathbf{h} \right\|_2^2, \tag{27}$$

where $\mathbf{y} = \text{vec}(\mathbf{Y})$ is given by (11) and $\mu \propto \sigma_w \sqrt{MN \log(MN)}$ is a weight factor [37]. Using (22), (27) can be equivalently formulated as a semi-definite program (SDP):

$$\min_{\substack{\mathcal{U}_4 \in \mathbb{C}^{(2N_1-1) \times (2N_2-1) \times (2M_1-1) \times (2M_2-1)}, \\ \mathbf{h} \in \mathbb{C}^{MN}, \ t \in \mathbb{R}}} \frac{\mu}{2MN} \text{Tr} \left( \mathbb{T}_4(\mathcal{U}_4) \right) + \frac{\mu}{2} t + \frac{1}{2} \left\| \mathbf{y} - \sqrt{P_t} \left( \mathbf{P}^T \otimes \mathbf{I}_M \right) \mathbf{h} \right\|_2^2$$

$$\text{s.t} \quad \begin{bmatrix} \mathbb{T}_4(\mathcal{U}_4) & \mathbf{h} \\ \mathbf{h}^H & t \end{bmatrix} \succeq 0. \tag{28}$$

The above problem is convex, and can be solved by using a standard convex solver. Suppose the solution to (28) is $\hat{\mathbf{h}}$. Then the estimated channel matrix is given by $\hat{\mathbf{H}} = \text{vec}^{-1} \left( \hat{\mathbf{h}} \right)$ where $\text{vec}^{-1}(\cdot)$ is the inverse operation of $\text{vec}(\cdot)$.

## IV. EFFICIENT ALGORITHM FOR CHANNEL ESTIMATION UNDER UPA

### A. A Formulation Based on 2D MMV Atomic Norm

Note that the dimension of the positive semidefinite matrix in (28) is $(MN + 1) \times (MN + 1)$, and the 4D atomic norm minimization formulation is of high computational complexity and has

large memory requirements. To reduce the complexity, we can treat $\mathbf{Y}$ as 2D multiple measurement vectors (MMV) [32] in transmit and receive dimensions.

Unlike the 4D atomic norm that is calculated with input vector $\mathbf{h}$, the MMV atomic norm is calculated with the matrix input $\mathbf{H}$. Specifically, we define the atom $\bar{\mathbf{Q}}(\mathbf{f}, \bar{\mathbf{a}}) = \mathbf{b}(\mathbf{f})\bar{\mathbf{a}}^H$ with $\mathbf{f} \in [-\frac{1}{2}, \frac{1}{2}) \times [-\frac{1}{2}, \frac{1}{2})$, and $\bar{\mathbf{a}} \in \mathbb{C}^{N\times1}$ with $\|\bar{\mathbf{a}}\|_2 = 1$. Correspondingly, the atom set is defined as

$$\mathcal{A}_{\text{MMV}} = \left\{ \bar{\mathbf{Q}}(\mathbf{f}, \bar{\mathbf{a}}) : \mathbf{f} \in [-\frac{1}{2}, \frac{1}{2}) \times [-\frac{1}{2}, \frac{1}{2}), \|\bar{\mathbf{a}}\|_2 = 1 \right\}. \tag{29}$$

It is worth noting that $\bar{\mathbf{a}}$ is not restricted by the structural constraint in (3). With (29), we extend the 1D MMV atomic norm [32] to the 2D MMV atomic norm of $\mathbf{H}$ defined by

$$\|\mathbf{H}\|_{\mathcal{A}_{\text{MMV}}} = \inf_{\substack{\mathbf{f}_l \in [-\frac{1}{2}, \frac{1}{2}) \times [-\frac{1}{2}, \frac{1}{2}), \\ \bar{\mathbf{a}}_l \in \mathbb{C}^{N\times1}, \ \sigma_l \in \mathbb{C}}} \left\{ \sum_l |\sigma_l| \ \middle| \ \mathbf{H} = \sum_l \sigma_l \bar{\mathbf{Q}}(\mathbf{f}_l, \bar{\mathbf{a}}_l), \|\bar{\mathbf{a}}\|_2 = 1 \right\}. \tag{30}$$

This atomic norm is equivalent to the solution of the following SDP [32]:

$$\|\mathbf{H}\|_{\mathcal{A}_{\text{MMV}}} = \inf_{\mathbf{U}_2 \in \mathbb{C}^{(2M_2-1)\times(2M_1-1)}, \mathbf{X} \in \mathbb{C}^{N\times N}} \left\{ \begin{array}{c} \frac{1}{2M}\text{Tr}(\mathbb{T}_2(\mathbf{U}_2)) + \frac{1}{2N}\text{Tr}(\mathbf{X}) \\ \\ \text{s.t.} \begin{bmatrix} \mathbb{T}_2(\mathbf{U}_2) & \mathbf{H} \\ \mathbf{H}^H & \mathbf{X} \end{bmatrix} \succeq 0 \end{array} \right\}, \tag{31}$$

where $\mathbf{X}$ is constrained to be a Hermitian matrix. Then using (9), we can formulate the following optimization problem for channel estimation:

$$\hat{\mathbf{H}} = \min_{\mathbf{H} \in \mathbb{C}^{M\times N}} \mu\|\mathbf{H}\|_{\mathcal{A}_{\text{MMV}}} + \frac{1}{2}\left\|\sqrt{P_t}\mathbf{H}\mathbf{P} - \mathbf{Y}\right\|_F^2, \tag{32}$$

where $\|\cdot\|_F$ denotes matrix Frobenius norm. Plugging (31) into (32), the size of the positive semidefinite matrix in the constraint is $(M + N) \times (M + N)$, resulting in considerably lower computational complexity and memory requirement than (28).

## B. An Approximation to 4D Atomic Norm Minimization

Next we propose an approximation to the 4D atomic norm to reduce the computational complexity. In [38], the authors explore the approximation of 2D atomic norm to improve the efficiency. Here, we extend the results from 2D atomic norm to 4D atomic norm case. Similar to the 2D MMV atomic norm, the proposed approximation is calculated with input $\mathbf{H}$. From (1), $\mathbf{H}$ is the sum of

$\sigma_l \mathbf{b}(\mathbf{f}_l)\mathbf{a}(\mathbf{g}_l)^H$, in which both $\mathbf{a}(\mathbf{g}_l)$ and $\mathbf{b}(\mathbf{f}_l)$ are Fourier bases. Different from the vectorized atomic norm, we introduce the matrix atom $\mathbf{Q}(\mathbf{f}, \mathbf{g}) = \mathbf{b}(\mathbf{f})\mathbf{a}(\mathbf{g})^H$ and the matrix atom set

$$\mathcal{A}_M = \left\{ \mathbf{Q}(\mathbf{f}, \mathbf{g}) = \mathbf{b}(\mathbf{f})\mathbf{a}(\mathbf{g})^H : \mathbf{f} \in [-\frac{1}{2}, \frac{1}{2}) \times [-\frac{1}{2}, \frac{1}{2}), \mathbf{g} \in [-\frac{1}{2}, \frac{1}{2}) \times [-\frac{1}{2}, \frac{1}{2}) \right\}. \tag{33}$$

The matrix atomic norm is then given by

$$\|\mathbf{H}\|_{\mathcal{A}_M} = \inf_{\substack{\mathbf{f}_l \in [-\frac{1}{2}, \frac{1}{2}) \times [-\frac{1}{2}, \frac{1}{2}), \\ \mathbf{g}_l \in [-\frac{1}{2}, \frac{1}{2}) \times [-\frac{1}{2}, \frac{1}{2}), \\ \sigma_l \in \mathbb{C}}} \left\{ \sum_l |\sigma_l| \,\middle|\, \mathbf{H} = \sum_l \sigma_l \mathbf{Q}(\mathbf{f}_l, \mathbf{g}_l) \right\}. \tag{34}$$

The matrix atom set is composed of rank-one matrices, and hence it amounts to atomic norm of low rank matrices. Since the operator $\text{vec}(\cdot)$ is a one-to-one mapping and the mapping $\mathcal{A}_M \to \mathcal{A}$ is also one-to-one, it is straightforward to conclude that $\|\mathbf{H}\|_{\mathcal{A}_M} = \|\mathbf{h}\|_{\mathcal{A}}$. Hence, if the component frequencies satisfy the sufficient separation condition given by (25) and (26), we have $\|\mathbf{H}\|_{\mathcal{A}_M} = \sum_l |\sigma_l|$ by Theorem 1.

Finding the harmonic components via atomic norm is an infinite programming problem over all feasible $\mathbf{f}$ and $\mathbf{g}$, which is difficult. For better efficiency, we use $\text{SDP}(\mathbf{H})$ in the following Lemma to approximate $\|\mathbf{H}\|_{\mathcal{A}_M}$.

**Lemma 1.** *For $\mathbf{H}$ given by (1), we have $\|\mathbf{H}\|_{\mathcal{A}_M} \geq \text{SDP}(\mathbf{H}) \geq \|\mathbf{H}\|_{\mathcal{A}_{\text{MMV}}}$, where*

$$\text{SDP}(\mathbf{H}) \triangleq \inf_{\mathbf{U}_2 \in \mathbb{C}^{(2M_2-1)\times(2M_1-1)}, \mathbf{V}_2 \in \mathbb{C}^{(2N_2-1)\times(2N_1-1)}} \left\{ \begin{array}{c} \frac{1}{2M}\text{Tr}\left(\mathbb{T}_2(\mathbf{U}_2)\right) + \frac{1}{2N}\text{Tr}\left(\mathbb{T}_2(\mathbf{V}_2)\right) \\ \\ s.t. \begin{bmatrix} \mathbb{T}_2(\mathbf{U}_2) & \mathbf{H} \\ \mathbf{H}^H & \mathbb{T}_2(\mathbf{V}_2) \end{bmatrix} \succeq 0 \end{array} \right\}, \tag{35}$$

*with $\mathbb{T}_2(\mathbf{U}_2)$ and $\mathbb{T}_2(\mathbf{V}_2)$ being 2-level Toeplitz matrices defined in (18).*

*Proof.* The relation $\text{SDP}(\mathbf{H}) \geq \|\mathbf{H}\|_{\mathcal{A}_{\text{MMV}}}$ can be directly obtained from the definitions in (31) and (35). It remains to show $\|\mathbf{H}\|_{\mathcal{A}_M} \geq \text{SDP}(\mathbf{H})$. Denote

$$\tilde{\mathbf{a}}(\mathbf{g}_l, \omega_l) = \frac{1}{\sqrt{N}} e^{j2\pi\omega_l} \mathbf{c}_{N_1}^*(g_{l,1}) \otimes \mathbf{c}_{N_2}^*(g_{l,2}),$$
$$\tilde{\mathbf{b}}(\mathbf{f}_l, \chi_l) = \frac{1}{\sqrt{M}} e^{j2\pi\chi_l} \mathbf{c}_{M_1}(f_{l,1}) \otimes \mathbf{c}_{M_2}(f_{l,2}),$$

with $\omega_l \in [0, 2\pi]$ and $\chi_l \in [0, 2\pi]$ such that $\sigma_l = |\sigma_l| e^{j2\pi(\omega_l + \chi_l)}$. For any $\mathbf{H} = \sum_l \sigma_l \mathbf{b}(\mathbf{f}_l) \mathbf{a}(\mathbf{g}_l)^H$, if we set

$$\mathbf{U}_2 = [\mathbf{u}_1(-M_1 + 1), \mathbf{u}_1(-M_1 + 2), ..., \mathbf{u}_1(M_1 - 1)], \tag{36}$$

$$\mathbf{V}_2 = [\mathbf{v}_1(-N_1 + 1), \mathbf{v}_1(-N_1 + 2), ..., \mathbf{v}_1(N_1 - 1)], \tag{37}$$

where

$$\mathbf{u}_1(i) = \frac{1}{\sqrt{M}} \sum_l |\sigma_l| \tilde{\mathbf{c}}_{M_2}(f_{l,2}) e^{j2\pi(i-1)f_{l,1}}, \tag{38}$$

$$\mathbf{v}_1(i) = \frac{1}{\sqrt{N}} \sum_l |\sigma_l| \tilde{\mathbf{c}}_{N_2}^*(g_{l,2}) e^{-j2\pi(i-1)g_{l,1}}, \tag{39}$$

with $\tilde{\mathbf{c}}_n(x) = \frac{1}{\sqrt{n}} \left[ e^{j2\pi(1-n)x}, e^{j2\pi(2-n)x}, \cdots, e^{j2\pi(n-1)x} \right]^T \in \mathbb{C}^{2n \times 1}$, then the 2-level Toeplitz matrices $\mathbb{T}_2(\mathbf{U}_2)$ and $\mathbb{T}_2(\mathbf{V}_2)$ satisfy

$$\begin{aligned} \mathbb{T}_2(\mathbf{U}_2) &= \sum_l |\sigma_l| \mathbf{b}(\mathbf{f}_l) \mathbf{b}(\mathbf{f}_l)^H \\ &= \sum_l |\sigma_l| \tilde{\mathbf{b}}(\mathbf{f}_l, \chi_l) \tilde{\mathbf{b}}(\mathbf{f}_l, \chi_l)^H, \end{aligned} \tag{40}$$

$$\begin{aligned} \mathbb{T}_2(\mathbf{V}_2) &= \sum_l |\sigma_l| \mathbf{a}(\mathbf{g}_l) \mathbf{a}(\mathbf{g}_l)^H \\ &= \sum_l |\sigma_l| \tilde{\mathbf{a}}(\mathbf{g}_l, \omega_l) \tilde{\mathbf{a}}(\mathbf{g}_l, \omega_l)^H. \end{aligned} \tag{41}$$

Moreover, the matrix

$$\mathbf{M} = \begin{bmatrix} \mathbb{T}_2(\mathbf{U}_2) & \mathbf{H} \\ \mathbf{H}^H & \mathbb{T}_2(\mathbf{V}_2) \end{bmatrix} = \sum_l |\sigma_l| \begin{bmatrix} \tilde{\mathbf{b}}(\mathbf{f}_l, \chi_l) \\ \tilde{\mathbf{a}}(\mathbf{g}_l, \omega_l) \end{bmatrix} \begin{bmatrix} \tilde{\mathbf{b}}(\mathbf{f}_l, \chi_l) \\ \tilde{\mathbf{a}}(\mathbf{g}_l, \omega_l) \end{bmatrix}^H \tag{42}$$

is positive semidefinite, indicating that the constraints in (35) are satisfied. Note that $\mathrm{SDP}(\mathbf{H}) \leq \frac{1}{2M} \mathrm{Tr}(\mathbb{T}_2(\mathbf{U}_2)) + \frac{1}{2N} \mathrm{Tr}(\mathbb{T}_2(\mathbf{V}_2)) = \sum_l |\sigma_l|$ according to the definition in (35). Since this holds for any decomposition of $\mathbf{H}$, we obtain $\mathrm{SDP}(\mathbf{H}) \leq \|\mathbf{H}\|_{\mathcal{A}_M}$. $\square$

The above lemma shows that $\mathrm{SDP}(\mathbf{H})$ is a lower bound of the matrix atomic norm. Moreover, the following lemma states that if the component frequencies are sufficiently separated, then $\mathrm{SDP}(\mathbf{H})$ is equivalent to $\|\mathbf{H}\|_{\mathcal{A}_M}$.

**Lemma 2.** *If* (25)-(26) *hold, then* $\|\mathbf{H}\|_{\mathcal{A}_M} = \mathrm{SDP}(\mathbf{H})$.
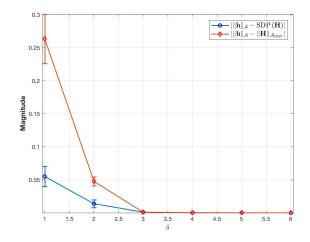
Figure 1: The approximation errors $\left|\|\mathbf{H}\|_{\mathcal{A}_M} - \text{SDP}(\mathbf{H})\right|$ and $\left|\|\mathbf{H}\|_{\mathcal{A}_M} - \|\mathbf{H}\|_{\mathcal{A}_{\text{MMV}}}\right|$ when the separations satisfy $\Delta_{\min,f_i} \geq \delta(M_i - 1)$, $\Delta_{\min,g_i} \geq \delta/(N_i - 1)$, $N_i = M_i = 16$, for $i = 1, 2$. The simulations are run 100 times for each $\delta$.

*Proof.* First it follows from Theorem 4 in [32] that if (25)-(26) hold, then we have $\|\mathbf{H}\|_{\mathcal{A}_{\text{MMV}}} = \sum_l |\sigma_l|$. Using Theorem 1 and the fact that $\|\mathbf{h}\|_{\mathcal{A}} = \|\mathbf{H}\|_{\mathcal{A}_M}$, we have $\|\mathbf{H}\|_{\mathcal{A}_M} = \|\mathbf{H}\|_{\mathcal{A}_{\text{MMV}}}$. Finally by Lemma 1 we have $\|\mathbf{H}\|_{\mathcal{A}_M} = \|\mathbf{H}\|_{\mathcal{A}_{\text{MMV}}} = \text{SDP}(\mathbf{H})$. $\square$

When the sufficient separation condition given by (25) and (26) is not satisfied, $\text{SDP}(\mathbf{H})$ may not be the same as $\|\mathbf{H}\|_{\mathcal{A}_M}$. However, it is found via simulations that $\text{SDP}(\mathbf{H})$ still provides a good approximation to $\|\mathbf{H}\|_{\mathcal{A}_M}$ and usually results in good performance in channel estimation. Moreover, as shown by Lemma 1, $\text{SDP}(\mathbf{H})$ is a lower bound of the atomic norm $\|\mathbf{H}\|_{\mathcal{A}_M}$ (or $\|\mathbf{h}\|_{\mathcal{A}}$ equivalently), i.e., $\|\mathbf{h}\|_{\mathcal{A}} = \|\mathbf{H}\|_{\mathcal{A}_M} \geq \text{SDP}(\mathbf{H})$ in general.

To show the approximation performances of both $\|\mathbf{H}\|_{\mathcal{A}_{\text{MMV}}}$ and $\text{SDP}(\mathbf{H})$ to $\|\mathbf{h}\|_{\mathcal{A}}$, we perform a series of Monte Carlo trials for parameters $M_1 = M_2 = 16$, $N_1 = N_2 = 16$ with $L = 2$. $\mathbf{f}_l$ and $\mathbf{g}_l$ take random values from $[-\frac{1}{2}, \frac{1}{2}) \times [-\frac{1}{2}, \frac{1}{2})$ such that the separations satisfy $\Delta_{\min,f_i} \geq \delta/\lfloor(N_i - 1)\rfloor$, $\Delta_{\min,g_i} \geq \delta/\lfloor(N_i - 1)\rfloor$ with $1 \leq \delta \leq 6$. In Fig. 1, we plot the approximation error against $\delta$ and the bars show $95\%$ confidence interval. As $\delta$ decreases, both approximation errors become larger. However, $\text{SDP}(\mathbf{H})$ provides a more accurate approximation than $\|\mathbf{H}\|_{\mathcal{A}_{\text{MMV}}}$. When $\delta \geq 4$, both approximation errors become zero.

Therefore, instead of solving the original 4D atomic norm minimization in (28), we can solve the following SDP

$$\hat{\mathbf{H}} = \min_{\substack{\mathbf{H}\in\mathbb{C}^{M\times N}, \\ \mathbf{U}_2\in\mathbb{C}^{(2M_2-1)\times(2M_1-1)}, \\ \mathbf{V}_2\in\mathbb{C}^{(2N_2-1)\times(2N_1-1)}}} \frac{\mu}{2M}\mathrm{Tr}\left(\mathbb{T}_2(\mathbf{U}_2)\right) + \frac{\mu}{2N}\mathrm{Tr}\left(\mathbb{T}_2(\mathbf{V}_2)\right) + \frac{1}{2}\left\|\sqrt{\mathrm{P}_t}\mathbf{H}\mathbf{P}-\mathbf{Y}\right\|_{\mathrm{F}}^2 \quad (43)$$

$$\text{s.t.} \quad \mathbf{M} = \begin{bmatrix} \mathbb{T}_2(\mathbf{U}_2) & \mathbf{H} \\ \mathbf{H}^H & \mathbb{T}_2(\mathbf{V}_2) \end{bmatrix} \succeq 0.$$

The size of the positive semidefinite matrix in the constraint is $(M+N)\times(M+N)$, resulting in considerably lower computational complexity and memory requirement than (28).

## C. ADMM for Approximate 4D Atomic Norm Minimization

To meet the requirement of real-time signal processing, we next derive an iterative algorithm for solving the SDP in (43), based on the alternating direction method of multipliers (ADMM) [39]. To put our problem in an appropriate form for ADMM, rewrite (43) as

$$\arg\min_{\substack{\mathbf{H}\in\mathbb{C}^{M\times N}, \\ \mathbf{U}_2\in\mathbb{C}^{(2M_2-1)\times(2M_1-1)}, \\ \mathbf{V}_2\in\mathbb{C}^{(2N_2-1)\times(2N_1-1)}}} \frac{1}{2}\|\mathbf{H}\mathbf{P}-\mathbf{Y}\|_F^2 + \frac{\gamma}{2M}\mathrm{Tr}\left(\mathbb{T}_2(\mathbf{U}_2)\right) + \frac{\gamma}{2N}\mathrm{Tr}\left(\mathbb{T}_2(\mathbf{V}_2)\right) + \mathbb{I}_\infty(\mathbf{M}\succeq\mathbf{0}), \quad (44)$$

where $\mathbb{I}_\infty(z)$ is an indicator function that is 0 if $z$ is true, and infinity otherwise. Dualize the equality constraint via an augmented Lagrangian, we have

$$\begin{aligned} \mathcal{L}_\rho(\mathbf{U}_2,\mathbf{V}_2,\mathbf{H},\boldsymbol{\Upsilon},\mathbf{M}) &= \frac{\gamma}{2M}\mathrm{Tr}\left(\mathbb{T}_2(\mathbf{U}_2)\right) + \frac{\gamma}{2N}\mathrm{Tr}\left(\mathbb{T}_2(\mathbf{V}_2)\right) + \frac{1}{2}\|\mathbf{H}\mathbf{P}-\mathbf{Y}\|_F^2 + \mathbb{I}_\infty(\mathbf{M}\succeq\mathbf{0}) \\ &\quad + \left\langle \boldsymbol{\Upsilon}, \mathbf{M} - \begin{bmatrix} \mathbb{T}_2(\mathbf{U}_2) & \mathbf{H} \\ \mathbf{H}^H & \mathbb{T}_2(\mathbf{V}_2) \end{bmatrix} \right\rangle \\ &\quad + \frac{\rho}{2}\left\| \mathbf{M} - \begin{bmatrix} \mathbb{T}_2(\mathbf{U}_2) & \mathbf{H} \\ \mathbf{H}^H & \mathbb{T}_2(\mathbf{V}_2) \end{bmatrix} \right\|_F^2, \end{aligned} \quad (45)$$

where $\mathbf{\Upsilon}$ is the dual variable, $\langle \mathbf{\Upsilon}, \mathbf{M} \rangle \triangleq \mathrm{Re}\left(\mathrm{Tr}(\mathbf{M}^H \mathbf{\Upsilon})\right)$, $\rho > 0$ is the penalty parameter. The ADMM consists of the following update steps:

$$(\mathbf{U}_2^{l+1}, \mathbf{V}_2^{l+1}, \mathbf{H}^{l+1}) = \arg \min_{\substack{\mathbf{H} \in \mathbb{C}^{M \times N}, \\ \mathbf{U}_2 \in \mathbb{C}^{(2M_2-1) \times (2M_1-1)}, \\ \mathbf{V}_2 \in \mathbb{C}^{(2N_2-1) \times (2N_1-1)}}} \mathcal{L}_\rho(\mathbf{U}_2, \mathbf{V}_2, \mathbf{H}, \mathbf{\Upsilon}^l, \mathbf{M}^l), \tag{46}$$

$$\mathbf{M}^{l+1} = \arg \min_{\mathbf{M} \in \mathbb{C}^{(M+N) \times (M+N)} \succeq 0} \mathcal{L}_\rho(\mathbf{U}_2^{l+1}, \mathbf{V}_2^{l+1}, \mathbf{H}^{l+1}, \mathbf{\Upsilon}^l, \mathbf{M}), \tag{47}$$

$$\mathbf{\Upsilon}^{l+1} = \mathbf{\Upsilon}^l + \rho \left( \mathbf{M}^{l+1} - \begin{bmatrix} \mathbb{T}_2(\mathbf{U}_2^{l+1}) & \mathbf{H}^{l+1} \\ (\mathbf{H}^{l+1})^H & \mathbb{T}_2(\mathbf{V}_2^{l+1}) \end{bmatrix} \right). \tag{48}$$

Now we derive the updates of (46) and (47) in detail. For convenience, the following partitions are introduced:

$$\mathbf{M}^l = \begin{bmatrix} \mathbf{M}_0^l & \mathbf{M}_2^l \\ (\mathbf{M}_2^l)^H & \mathbf{M}_1^l \end{bmatrix}, \tag{49}$$

$$\mathbf{\Upsilon}^l = \begin{bmatrix} \mathbf{\Upsilon}_0^l & \mathbf{\Upsilon}_2^l \\ (\mathbf{\Upsilon}_2^l)^H & \mathbf{\Upsilon}_1^l \end{bmatrix}, \tag{50}$$

where $\mathbf{M}_0^l$ and $\mathbf{\Upsilon}_0^l$ are $M \times M$ matrices, $\mathbf{M}_2^l$ and $\mathbf{\Upsilon}_2^l$ are $M \times N$ matrices, $\mathbf{M}_1^l$ and $\mathbf{\Upsilon}_1^l$ are $N \times N$ matrices. Computing the derivative of $\mathcal{L}_\rho(\mathbf{U}_2, \mathbf{V}_2, \mathbf{H}, \mathbf{\Upsilon}, \mathbf{M})$ with respect to $\mathbf{H}$, $\mathbf{U}_2$ and $\mathbf{V}_2$, we have

$$\nabla_{\mathbf{H}} \mathcal{L}_\rho = (\mathbf{H}\mathbf{P} - \mathbf{Y})\mathbf{P}^H - 2\mathbf{\Upsilon}_2^l + 2\rho(\mathbf{H} - \mathbf{M}_2^l), \tag{51}$$

$$\nabla_{U_2(i,k)} \mathcal{L}_\rho = \begin{cases} \frac{\gamma}{2} + M_1 \rho U_2(i,k) - \mathrm{Tr}(\rho \mathbf{M}_0^l + \mathbf{\Upsilon}_0^l), & i = k = 0, \\ (M_1 - i)(M_2 - k)\rho U_2(i,k) - \sum_{m=0}^{M_2-i-1} \mathrm{Tr}_k\left(\mathcal{S}_{i,k}^{(1)}(\rho \mathbf{M}_0^l + \mathbf{\Upsilon}_0^l)\right), & i \neq 0 \text{ or } k \neq 0, \end{cases} \tag{52}$$

$$\nabla_{V_2(i,k)} \mathcal{L}_\rho = \begin{cases} \frac{\gamma}{2} + N_1 \rho V_2(i,k) - \mathrm{Tr}(\rho \mathbf{M}_1^l + \mathbf{\Upsilon}_1^l), & i = k = 0, \\ (N_1 - i)(N_2 - k)\rho V_2(i,k) - \sum_{m=0}^{N_2-i-1} \mathrm{Tr}_k\left(\mathcal{S}_{i,k}^{(2)}(\rho \mathbf{M}_1^l + \mathbf{\Upsilon}_1^l)\right), & i \neq 0 \text{ or } k \neq 0, \end{cases} \tag{53}$$

where $U_2(i,k)$ and $V_2(i,k)$ are the $(i,k)$-th elements of $\mathbf{U}_2$ and $\mathbf{V}_2$, respectively. For $\mathbf{X} \in \mathbb{C}^{M \times M}$, $\mathcal{S}_{i,k}^{(1)}(\mathbf{X})$ returns the $(i,k)$-th $M_1 \times M_1$ submatrix $\mathbf{X}_{i,k}$. For $\mathbf{X} \in \mathbb{C}^{N \times N}$, $\mathcal{S}_{i,k}^{(2)}(\mathbf{X})$ returns the $(i,k)$-th $N_1 \times N_1$ submatrix $\mathbf{X}_{i,k}$. $\mathrm{Tr}_k(\cdot)$ outputs the trace of the $k$-th sub-diagnal of the input matrix. $\mathrm{Tr}_0(\cdot)$ outputs the trace of the input matrix.

By setting the derivatives to 0, $\mathbf{H}^{l+1}$, $\mathbf{U}_2^{l+1}$ and $\mathbf{V}_2^{l+1}$ can be updated by:

$$\mathbf{H}^{l+1} = (\mathbf{Y}\mathbf{P}^H + 2\rho\mathbf{M}_2^l + 2\mathbf{\Upsilon}_2^l)(\mathbf{P}\mathbf{P}^H + 2\rho\mathbf{I}_N)^{-1}, \tag{54}$$

$$\mathbf{U}_2^{l+1} = \mathbb{T}_2^*(\mathbf{M}_0^l + \mathbf{\Upsilon}_0^l/\rho) - \frac{\gamma}{2M\rho}\mathbf{e}_1, \tag{55}$$

$$\mathbf{V}_2^{l+1} = \mathbb{T}_2^*(\mathbf{M}_1^l + \mathbf{\Upsilon}_1^l/\rho) - \frac{\gamma}{2N\rho}\mathbf{e}_1, \tag{56}$$

where $\mathbf{e}_1 = [1,0,0,...,0]^T$, $\mathbb{T}_2^*(\cdot)$ denotes the adjoints of the map $\mathbb{T}_2(\cdot)$. Specifically, suppose $\mathbf{Z} = \mathbb{T}_2^*(\mathbf{X})$ where $\mathbf{Z} = [\mathbf{z}_{-M_2+1}, \mathbf{z}_{-M_2+2}, ..., \mathbf{z}_{M_2-1}]$ with $\mathbf{z}_i = [z_i(-M_1+1), z_i(-M_1+2), ..., z_i(M_1-1)]^T$ when $\mathbf{X} \in \mathbb{C}^{M \times M}$. Then we have

$$z_i(k) = \frac{1}{(M_1-i)(M_2-k)} \sum_{m=0}^{M_1-i-1} \text{Tr}_k(\mathcal{S}_{i,m}^{(1)}(\mathbf{X})), \tag{57}$$

for $i = -M_2 + 1, -M_2 + 2, ..., M_2 - 1$ and $k = -M_1 + 1, -M_1 + 2, ..., M_1 - 1$.

The update of $\mathbf{M}$ is given by

$$\mathbf{M}^{l+1} = \arg \min_{\mathbf{M} \in \mathbb{C}^{(M+N)\times(M+N)} \succeq 0} \left\| \mathbf{M} - \tilde{\mathbf{M}}^{l+1} \right\|_F^2, \tag{58}$$

where

$$\tilde{\mathbf{M}}^{l+1} = \begin{bmatrix} \mathbb{T}_2(\mathbf{U}_2^{l+1}) & \mathbf{H}^{l+1} \\ (\mathbf{H}^{l+1})^H & \mathbb{T}_2(\mathbf{V}_2^{l+1}) \end{bmatrix} - \mathbf{\Upsilon}^{l+1}/\rho. \tag{59}$$

It is equivalent to projecting $\tilde{\mathbf{M}}^{l+1}$ onto the positive semidefinite cone. Specifically, the projection is accomplished by setting all negative eigenvalues of $\tilde{\mathbf{M}}^{l+1}$ to zero. Note that in ADMM the update of variables $\mathbf{H}$, $\mathbf{U}_2$, $\mathbf{V}_2$ and $\mathbf{M}$ are in closed-form. Compared to the off-the-shelf solvers such as SeDuMi [40] and SDPT3 [41], whose computational complexity is $\mathcal{O}\left((M+N)^6\right)$ in each iteration, the complexity of ADMM is $\mathcal{O}\left((M+N)^3\right)$ in each iteration, so it runs much faster.

## V. THE GENERAL PLANAR ARRAY CASE

So far we have focused on the uniform planar array (UPA). For mmWave beamformed FD-MIMO, because of the larger average inter-antenna element spacing, non-uniform planar array (NUPA) requires fewer elements than UPA, whereby reducing the weight and cost of the system in large array applications. Also, the irregular spacing allows the antenna grid spacing to become larger than a half wavelength so it can effectively reduce the channel correlation and enhance multiplexing

gain [42]. Furthermore, there is a fundamental limitation of UPA, namely, the lower resolution of elevation AoA, which limits the UPA performance [24].

In this section we consider the beamformed mmWave FD-MIMO channel estimation for NUPA. Define $\mathbf{d}_t = \frac{2}{\lambda} [(d_{t,1}(1), d_{t,2}(1)) \ldots (d_{t,1}(N), d_{t,2}(N))]$ as the normalized transmit antenna locations, where $(d_{t,1}(i), d_{t,2}(i))$ is the $i$-th transmit antenna coordinate in a 2D planar surface. Similarly, $\mathbf{d}_r = \frac{2}{\lambda} [(d_{r,1}(1), d_{r,2}(1)) \ldots (d_{r,1}(M), d_{r,2}(M))]$ is the normalized receive antenna locations where $(d_{r,1}(i), d_{r,2}(i))$ is the $i$-th receive antenna coordinate in a 2D planar surface. Then the steering responses of the transmit and receive arrays for the $l$-th path can be respectively written as [43]

$$\mathbf{a}_{\mathbf{d}_t}(\mathbf{g}_l) = \frac{1}{\sqrt{N}} \left[ e^{j2\pi \left( \frac{2d_{t,1}(1)}{\lambda} g_{l,1} + \frac{2d_{t,2}(1)}{\lambda} g_{l,2} \right)} \ldots e^{j2\pi \left( \frac{2d_{t,1}(N)}{\lambda} g_{l,1} + \frac{2d_{t,2}(N)}{\lambda} g_{l,2} \right)} \right]^T, \tag{60}$$

$$\mathbf{b}_{\mathbf{d}_r}(\mathbf{f}_l) = \frac{1}{\sqrt{M}} \left[ e^{j2\pi \left( \frac{2d_{r,1}(1)}{\lambda} f_{l,1} + \frac{2d_{r,2}(1)}{\lambda} f_{l,2} \right)} \ldots e^{j2\pi \left( \frac{2d_{r,1}(M)}{\lambda} f_{l,1} + \frac{2d_{r,2}(M)}{\lambda} f_{l,2} \right)} \right]^T. \tag{61}$$

With (60) and (61), the channel matrix $\mathbf{H}$ of NUPA is given by (1) with array responses $\mathbf{a}(\mathbf{g}_l)$ and $\mathbf{b}(\mathbf{f}_l)$ replaced by $\mathbf{a}_{\mathbf{d}_t}(\mathbf{g}_l)$ and $\mathbf{b}_{\mathbf{d}_r}(\mathbf{f}_l)$, respectively.

The atom for NUPA is then defined as

$$\mathbf{q}_{\mathrm{NU}}(\mathbf{g}, \mathbf{f}) = \mathbf{a}_{\mathbf{d}_t}^*(\mathbf{g}) \otimes \mathbf{b}_{\mathbf{d}_r}(\mathbf{f}). \tag{62}$$

And the atom set for NUPA is given by

$$\mathcal{A}_{\mathrm{NU}} \triangleq \left\{ \mathbf{q}_{\mathrm{NU}}(\mathbf{g}, \mathbf{f}), \mathbf{g} \in [\frac{-1}{2}, \frac{1}{2}) \times [-\frac{1}{2}, \frac{1}{2}), \mathbf{f} \in [\frac{-1}{2}, \frac{1}{2}) \times [\frac{-1}{2}, \frac{1}{2}) \right\}. \tag{63}$$

The atomic norm $\|\mathbf{h}\|_{\mathcal{A}_{\mathrm{NU}}}$ for any $\mathbf{h} = \mathrm{vec}(\mathbf{H})$ is then given by

$$\|\mathbf{h}\|_{\mathcal{A}_{\mathrm{NU}}} = \inf_{\substack{\mathbf{f}_l \in [-\frac{1}{2}, \frac{1}{2}) \times [-\frac{1}{2}, \frac{1}{2}), \\ \mathbf{g}_l \in [-\frac{1}{2}, \frac{1}{2}) \times [-\frac{1}{2}, \frac{1}{2}), \\ \sigma_l \in \mathbb{C}}} \left\{ \sum_l |\sigma_l| \, \middle| \, \mathbf{h} = \sum_l \sigma_l \mathbf{q}_{\mathrm{NU}}(\mathbf{g}_l, \mathbf{f}_l) \right\}. \tag{64}$$

To estimate the channel, we propose to solve the following optimization problem

$$\min_{\mathbf{h}} \mu \|\mathbf{h}\|_{\mathcal{A}_{\mathrm{NU}}} + \frac{1}{2} \left\| \mathbf{y} - \sqrt{P_t} \left( \mathbf{P}^T \otimes \mathbf{I}_M \right) \mathbf{h} \right\|_2^2. \tag{65}$$

Note that the atom defined in (62) is not based on uniform sampling, and consequently the atomic norm in (64) does not have the equivalent SDP form as in (28) or (43). Hence, (65) cannot be solved

via convex optimization. According to Corollary 2.1 of [44], (65) shares the same optimum as the following optimization problem

$$\min_{\substack{\mathbf{f}_l \in [-\frac{1}{2}, \frac{1}{2}) \times [-\frac{1}{2}, \frac{1}{2}), \\ \mathbf{g}_l \in [-\frac{1}{2}, \frac{1}{2}) \times [-\frac{1}{2}, \frac{1}{2}), \\ \sigma_l \in \mathbb{C}}} \Gamma\left(\{\mathbf{g}_l, \mathbf{f}_l, \sigma_l\}\right) = \mu \|\boldsymbol{\sigma}\|_1 + \frac{1}{2} \left\| \mathbf{y} - \sqrt{P_t} \left(\mathbf{P}^T \otimes \mathbf{I}_M\right) \sum_{l=1}^{L} \mathbf{q}_{\mathrm{NU}}\left(\mathbf{g}_l, \mathbf{f}_l\right) \sigma_l \right\|_2^2. \quad (66)$$

Since the problem given by (66) is nonconvex, we will employ a gradient-descent algorithm to obtain its local optimum. In practice, $L$ is unknown, so we initialize $\mathbf{q}\left(\mathbf{g}_l, \mathbf{f}_l\right)$ on $\tilde{L}^0$ grid points such that $L \leq \tilde{L}^0 \leq MP$, where $P$ is the number of training beams defined in (8). For example, let each $\mathbf{g}_l$ and $\mathbf{f}_l$ be taken from a uniform grid of $N_G$ points with $\tilde{L}^0 = N_G^4 \leq MP$, i.e., $g_{l,i}^0$ and $f_{l,i}^0$ are uniformly taken from $[-1/2, 1/2)$ for $i = 1, 2$ and $1 \leq l \leq N_G^4$, where the supercript $^0$ indicates iteration 0, i.e., initialization. Let $\boldsymbol{\Omega}^0 = \left\{ (\mathbf{g}_l^0, \mathbf{f}_l^0)_{1 \leq l \leq \tilde{L}} \right\}$. The initial value of $\boldsymbol{\sigma}^0 = \left[\sigma_1^0 \ldots \sigma_{\tilde{L}}^0\right]^T$ can then be obtained by the least-squares (LS) estimate

$$\boldsymbol{\sigma}^0 = \left(\left(\mathbf{P}^T \otimes \mathbf{I}_M\right) \left[\mathbf{q}_{\mathrm{NU}}\left(\mathbf{g}_1^0, \mathbf{f}_1^0\right) \ldots \mathbf{q}_{\mathrm{NU}}\left(\mathbf{g}_{\tilde{L}}^0, \mathbf{f}_{\tilde{L}}^0\right)\right]\right)^\dagger \mathbf{y}, \quad (67)$$

where $^\dagger$ indicates the pseudo inverse of the matrix. Then the gradient descent method is used to find the local optimum. We use superscript $k$ to denote the quantities in the $k$-th iteration. Then the gradient descent search proceeds as follows

$$g_{l,i}^{k+1} = \left[g_{l,i}^k - \kappa^k \nabla_{g_{l,i}} \Gamma\left(\{\mathbf{g}_l^k, \mathbf{f}_l^k, \sigma_l^k\}\right)\right]_{-\frac{1}{2}}^{\frac{1}{2}}, \quad (68)$$

$$f_{l,i}^{k+1} = \left[f_{l,i}^k - \kappa^k \nabla_{f_{l,i}} \Gamma\left(\{\mathbf{g}_l^k, \mathbf{f}_l^k, \sigma_l^k\}\right)\right]_{-\frac{1}{2}}^{\frac{1}{2}}, \quad (69)$$

$$\sigma_l^{k+1} = \sigma_l^k - \kappa^k \nabla_{\sigma_l} \Gamma\left(\{\mathbf{g}_l^k, \mathbf{f}_l^k, \sigma_l^k\}\right), \quad (70)$$

for $l = 1, \ldots, \tilde{L}^k$ and $i = 1, 2$, where $\kappa^k$ is the step size that can be obtained via Armijo line search [45] and $[x]_b^a$ defines the operator that outputs $x = \mod(x, a)$ when $x < b$, and outputs $x = \mod(x, b)$ when $x > a$, $\mod(a, b)$ defines the modulo operator. Specifically, in the $k$-th iteration, $\kappa^k$ is initialized as $\kappa^k = \bar{\kappa}$. If $\Gamma\left(\{\mathbf{g}_l^{k+1}, \mathbf{f}_l^{k+1}, \sigma_l^{k+1}\}\right) \geq \Gamma\left(\{\mathbf{g}_l^k, \mathbf{f}_l^k, \sigma_l^k\}\right)$, then $\kappa^k$ is updated by

multiplication with a constant $0 < \alpha < 1$, i.e., $\kappa^k \leftarrow \alpha\kappa^k$. The gradients are calculated

$$\nabla_{g_{l,i}}\Gamma\left(\{\mathbf{g}_l, \mathbf{f}_l, \sigma_l\}\right) = \mathcal{R}\left\{\sigma_l\left(\bar{\mathbf{P}}\sum_{l=1}^{\tilde{L}}\mathbf{q}_{\mathrm{NU}}\left(\mathbf{g}_l, \mathbf{f}_l\right)\sigma_l - \mathbf{y}\right)^H \bar{\mathbf{P}}\left(\mathbf{a}_{\mathbf{d}_{t,i}}^*\left(\mathbf{g}_l\right) \otimes \mathbf{b}_{\mathbf{d}_r}\left(\mathbf{f}_l\right)\right)\right\}, \quad (71)$$

$$\nabla_{f_{l,i}}\Gamma\left(\{\mathbf{g}_l, \mathbf{f}_l, \sigma_l\}\right) = \mathcal{R}\left\{\sigma_l\left(\bar{\mathbf{P}}\sum_{l=1}^{\tilde{L}}\mathbf{q}_{\mathrm{NU}}\left(\mathbf{g}_l, \mathbf{f}_l\right)\sigma_l - \mathbf{y}\right)^H \bar{\mathbf{P}}\left(\mathbf{a}_{\mathbf{d}_t}^*\left(\mathbf{g}_l\right) \otimes \mathbf{b}_{\mathbf{d}_{r,i}}\left(\mathbf{f}_l\right)\right)\right\}, \quad (72)$$

$$\nabla_{\sigma_l}\Gamma\left(\{\mathbf{g}_l, \mathbf{f}_l, \sigma_l\}\right) = \mu\frac{\sigma_l}{2|\sigma_l|} + \frac{1}{2}\left(\bar{\mathbf{P}}\sum_{l=1}^{\tilde{L}}\mathbf{q}_{\mathrm{NU}}\left(\mathbf{g}_l, \mathbf{f}_l\right)\sigma_l - \mathbf{y}\right)^T\left(\bar{\mathbf{P}}\mathbf{q}_{\mathrm{NU}}\left(\mathbf{g}_l, \mathbf{f}_l\right)\right)^*, \quad (73)$$

where $\mathcal{R}\left\{\cdot\right\}$ returns the real part of the input,

$$\bar{\mathbf{P}} = \sqrt{P_t}\left(\mathbf{P}^T \otimes \mathbf{I}_M\right), \quad (74)$$

$$\mathbf{a}_{\mathbf{d}_{t,i}}\left(\mathbf{g}_l\right) = \left(\frac{j2\pi}{\lambda}\left[d_{t,i}(1), \ldots, d_{t,i}(N)\right]^T\right) \circ \mathbf{a}_{\mathbf{d}_t}\left(\mathbf{g}_l\right), \quad (75)$$

$$\mathbf{b}_{\mathbf{d}_{r,i}}\left(\mathbf{f}_l\right) = \left(\frac{j2\pi}{\lambda}\left[d_{r,i}(1), \ldots, d_{r,i}(M)\right]^T\right) \circ \mathbf{b}_{\mathbf{d}_r}\left(\mathbf{f}_l\right), \quad (76)$$

and $\circ$ denotes Hadamard product. The derivations of (71) - (73) are given in the Appendix. To accelerate the convergence, we introduce a pruning step to remove the atoms whose coefficients are smaller than a threshold during each iteration. Specifically, at the $k$-th iteration, if $|\sigma_l^k| < \eta^k$ where $\eta^k$ is a given threshold at the $k$-th iteration, then $l$-th path are removed from the set and number of estimated paths is decreased by one, i.e., $\mathbf{\Omega}^k \leftarrow \mathbf{\Omega}^k \setminus \left\{\left(\mathbf{g}_l^k, \mathbf{f}_l^k\right)\right\}$ and $\tilde{L}^k \leftarrow \tilde{L}^k - 1$ at the $k$-th iteration. The algorithm stops when $\left\|\mathbf{h}^{k+1} - \mathbf{h}^k\right\| < \varepsilon$, where $\mathbf{h}^k = \sum_{l=1}^{\tilde{L}^k}\mathbf{q}_{\mathrm{NU}}\left(\mathbf{g}_l^k, \mathbf{f}_l^k\right)\sigma_l^k$ denotes the channel estimation at the $k$-th iteration.

## VI. Simulation Results

### A. Simulation Setup

In this section, we evaluate the performance of the proposed channel estimators for mmWave FD-MIMO links with UPA or NUPA. We compare the channel estimation performance of the proposed algorithm with some existing algorithms including the 4D-MUSIC [12] and the orthogonal matching pursuit (OMP) [46]. The simulation parameters are set as follows.

1, The numbers of transmit and receive antenna are $N = 16$ and $M = 16$, respectively. For UPA, we set $N_1 = 4$, $N_2 = 4$, $M_1 = 4$ and $M_2 = 4$.

2, In the UPA case, the DFT codebooks at the transmitter for elevation and azimuth are given by

$$\mathbf{P}_1 = \left[\mathbf{c}_{N_1}\left(\psi_{1,0}\right)\ \mathbf{c}_{N_1}\left(\psi_{1,1}\right)\cdots\mathbf{c}_{N_1}\left(\psi_{1,P_1-1}\right)\right] \in \mathbb{C}^{N_1\times P_1},$$

$$\mathbf{P}_2 = \left[\mathbf{c}_{N_2}\left(\psi_{2,0}\right)\ \mathbf{c}_{N_2}\left(\psi_{2,1}\right)\cdots\mathbf{c}_{N_2}\left(\psi_{2,P_2-1}\right)\right] \in \mathbb{C}^{N_2\times P_2},$$

where $P_1$ and $P_2$ are the sizes of elevation and azimuth codebooks, respectively. The DFT angles are $\psi_{1,i} = \frac{i}{P_1}$ for $i = 0,\ldots,P_1-1$ and $\psi_{2,i} = \frac{i}{P_2}$ for $i = 0,\ldots,P_2-1$. We take the Kronecker product of $\mathbf{P}_1$ and $\mathbf{P}_2$ to form the product codebook $\mathbf{P} = \mathbf{P}_1 \otimes \mathbf{P}_2$ with size $P = P_1 P_2$. Each beamforming vector has a unit norm, i.e., $\|\mathbf{p}_p\| = 1$ for $p = 1,\ldots,P$ and $\mathrm{rank}\left(\mathbf{P}\right) = P$.

3, The weight factor in (28) and (43) is set as $\mu = \sigma_w\sqrt{MN\log\left(MN\right)}$. The weight for the augmented Lagrangian in (45) is set as $\rho = 0.05$.

4, $\mathbf{g}_l$ and $\mathbf{f}_l$ for each path are assumed to uniformly take values in $[-\frac{1}{2},\frac{1}{2}) \times [-\frac{1}{2},\frac{1}{2})$. The number of paths $L = 3$.

5, The signal power is controlled by the signal-to-noise ratio (SNR) which is defined as $\mathrm{SNR} = \frac{P_t}{\sigma_w^2}$ with $\sigma_w^2 = 1$.

6, For NUPA, we use circular arrays for both transmitter and receiver with $N$ and $M$ antenna elements located on the 2D plane, respectively. Specifically, the $n$-th transmit antenna location is set as $d_{t,1}(n) = R_t\cos\left(\chi_n\right), d_{t,2}(n) = R_t\sin\left(\chi_n\right),\ n = 1,2,\ldots,N$, where $\chi_n = 2\pi\left(\frac{n}{N}\right)$ is the angular position of the $n$-th element and $R_t$ is the radius of the transmit array. Similarly, the $m$-th receive antenna location is $d_{r,1}(m) = R_r\cos\left(\chi_m\right), d_{r,2}(m) = R_r\sin\left(\chi_m\right),\ m = 1,2,\ldots,M$, where $\chi_m = 2\pi\left(\frac{m}{M}\right)$ is the angular position of the $m$-th element and $R_r$ is the radius of the receive array.

7, For the gradient descent algorithm, we set $\tilde{L}^0 = MP$ as the initial value in both UPA and NUPA cases. The pruning threshold in the $k$-th step is set as $\eta^k = 0.7\max_{1\le l\le \tilde{L}^k}\left\{\sigma_l^k\right\}$.

8, For the OMP and 4D-MUSIC algorithms, the AoD and AoA grid points are set as $\bar{\vartheta}_i = \frac{(i-1)2\pi}{N_G} - \pi$, $\bar{\varphi}_i = \frac{(i-1)2\pi}{N_G} - \pi$ and $\bar{\theta}_i = \frac{(i-1)2\pi}{N_G} - \pi$, $\bar{\phi}_i = \frac{(i-1)2\pi}{N_G} - \pi$, respectively, for $i = 1,\ldots N_G$.

9, In the simulation, we use the CVX package [47] to compute the 4D atomic norm-based estimator.

*B. Performance Evaluation*

We use the normalized mean square error (NMSE), i.e., NMSE $= \mathbb{E}\left\{\frac{\|\hat{\mathbf{H}}-\mathbf{H}\|_F^2}{\|\mathbf{H}\|_F^2}\right\}$ as the channel estimation performance metric. The NMSE statistics across different SNRs with different test setups are evaluated. Each curve is obtained by averaging over 100 realizations. First we compare the channel estimation performance of different algorithms under the UPA setting. Then we show the channel estimation performance for NUPA with the proposed gradient descent estimator and compare it with the 4D-MUSIC and OMP algorithms.

The computational complexity of the proposed approximate 4D atomic-norm-based channel estimator is $\mathcal{O}((M + N)^3)$ per-iteration. The computational complexity of the MUSIC estimator is $\mathcal{O}\left((NM)^3 + N_G^4 (NM)^2\right)$ where $\mathcal{O}\left((NM)^3\right)$ is for eigen decomposition and $\mathcal{O}\left(N_G^4 (NM)^2\right)$ is for grid search. The complexity of the OMP estimator is $\mathcal{O}\left(N_G^4 (NM)^2\right)$ per iteration. The complexity of proposed gradient descent estimator is $\mathcal{O}\left(M\left(N + P\right)\right)$ per iteration.

*1) Convergence Behavior of the Proposed Channel Estimators:* We illustrate the convergence of the proposed ADMM implementation of the approximate 4D atomic-norm-based channel estimator through a simulation example. We compare the NMSE of the ADMM channel estimator with that of the CVX solver [47] that directly solves (43). As can be seen from Fig. 2, the proposed ADMM channel estimator converges to the solution given by the CVX after 300-400 iterations for different SNR. It is worth noting that the ADMM runs much faster than the CVX solver because the calculation in each iteration is in closed-form. We then show the convergence behavior and the number of estimated paths of the proposed gradient-descent-based channel estimator for UPA and NUPA in Fig. 3. It is seen that the algorithm converges within 1500-2000 iterations for different SNR. The estimated number of paths is more accurate at higher SNR when the algorithm converges, as more spurious frequencies arise when the noise is stronger. It is also worth noting that the computational complexity of the gradient descent method is lower than that of the ADMM, but the overall running time is higher because it takes more iterations.

*2) Comparison of On-grid and Off-grid Algorithms:* We compare the proposed off-grid channel estimator with two existing on-grid approaches including OMP and MUSIC. For the on-grid algorithms, the continuous AoA and AoD parameter spaces are discretized into a finite set of grids
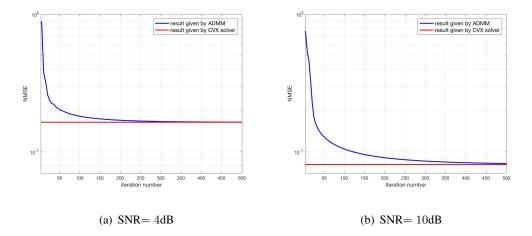
(a) SNR= 4dB

(b) SNR= 10dB

Figure 2: Convergence of proposed ADMM channel estimator with different SNR.

covering $[-\pi, \pi]$, and the estimation performance improves with higher grid resolution (i.e., larger $N_G$). However, higher grid resolution leads to higher computational complexity.

In Fig. 4, the NMSE and running time of different channel estimators are plotted against $N_G$. In this simulation, we use CVX solver to compute the 4D atomic-norm-based estimator and the ADMM algorithm to compute the approximate 4D atomic-norm-based estimator. It is worth noting that the proposed approximate 4D atomic-norm-based estimator has the smallest complexity while its NMSE is much smaller than those of the on-grid algorithms. As the algorithm does not require the grids, its computational complexity does not change with $N_G$. In addition, its NMSE performance is only slightly worse than the 4D atomic-norm-based channel estimator, indicating that the performance loss caused by the approximation of $\|\mathbf{H}\|_{\mathcal{A}_M}$ by SDP($\mathbf{H}$) is small.
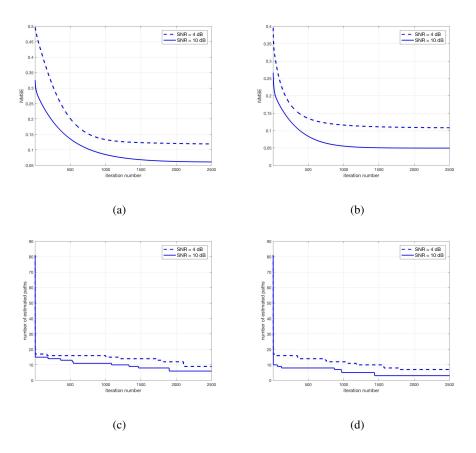
(a)

(b)

(c)

(d)

Figure 3: Convergence and the number of estimated paths of the proposed gradient descent algorithm for (a)(c) UPA and (b)(d) NUPA.
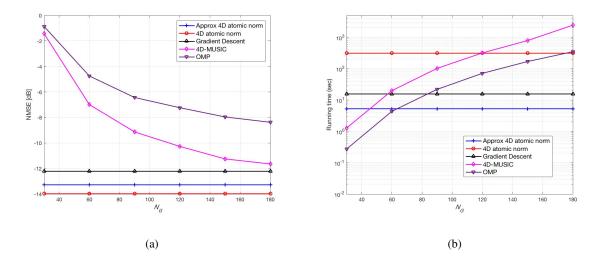


(a)

(b)

Figure 4: Comparison of channel estimation performance and running time against grid size, SNR= 10 dB. (a) NMSE performance; (b) running time.

*3) Channel Estimation Performance:* Fig. 5 plots the NMSE curves as a function of SNR for different channel estimators under UPA. The number of grid points are set as $N_G = 90, 180$ for 4D-MUSIC-based and OMP-based channel estimators.

It is seen that 4D atomic-norm-based and approximate 4D atomic-norm-based estimators outperform the 4D-MUSIC-based and OMP-based estimators. Meanwhile, the 4D atomic-norm-based channel estimator achieves better performance than the approximate 4D atomic-norm-based channel estimator by about from $0.5$ - $0.8$ dB. And the approximate 4D atomic-norm-based channel estimator outperforms the gradient-descent-based algorithm by more than $1.0$ dB.
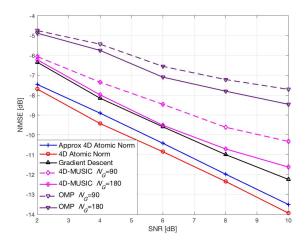


Figure 5: The NMSE performance as a function of SNR for UPA.

In Fig. 6, we plot the NMSE curves as a function of SNR for different channel estimators under NUPA. It is seen that the proposed gradient-descent-based channel estimator outperforms the 4D-MUSIC and OMP-based channel estimators across the range of SNRs from $2$ to $10$ dB. This is because the proposed gradient-descent-based channel estimator optimizes the frequency basis in each iteration, so it outperforms the on-grid algorithms.
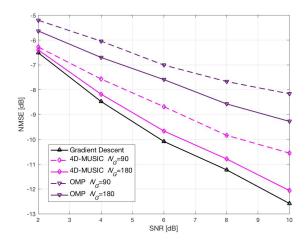
Figure 6: The NMSE performance as a function of SNR for NUPA.

## VII. CONCLUSIONS

In this paper, we have proposed new channel estimation schemes for mmWave beamformed FD-MIMO systems based on atomic norm minimization under both UPA and NUPA settings. For the UPA case, we approximate the original large-scale 4D atomic norm minimization problem using a semi-definite program (SDP) containing two decoupled two-level Toeplitz matrices which is then solved by an ADMM-based fast algorithm. For the NUPA case, a gradient descent-based algorithm is provided to obtain a suboptimal solution. Simulation results show that the proposed atomic norm based mmWave FD-MIMO channel estimators provide better performance compared to the existing methods based on compressed sensing and MUSIC algorithms.

## APPENDIX

### A. Derivation for (71) and (72)

For clarity, define $\bar{\mathbf{P}} = \sqrt{P_t}\left(\mathbf{P}^T \otimes \mathbf{I}_M\right)$. Then the gradient with respect to $g_{l,i}$ can be calculated by

$$\nabla_{g_{l,i}}\Gamma\left(\{\mathbf{g}_l, \mathbf{f}_l, \sigma_l\}\right) = \frac{1}{2}\frac{\partial\left(\mathbf{y} - \bar{\mathbf{P}}\mathbf{h}\right)^H\left(\mathbf{y} - \bar{\mathbf{P}}\mathbf{h}\right)}{\partial g_{l,i}} = \mathcal{R}\left\{\left(\bar{\mathbf{P}}\mathbf{h} - \mathbf{y}\right)^H\frac{\partial\bar{\mathbf{P}}\mathbf{h}}{\partial g_{l,i}}\right\}, \qquad (77)$$

where

$$\frac{\partial \bar{\mathbf{P}} \mathbf{h}}{\partial g_{l,i}} = \frac{\partial \bar{\mathbf{P}} \sum_{l=1}^{L} \mathbf{q}_{\text{NU}} (\mathbf{g}_l, \mathbf{f}_l) \sigma_l}{\partial g_{l,i}} = \sigma_l \bar{\mathbf{P}} \frac{\partial \mathbf{q}_{\text{NU}} (\mathbf{g}_l, \mathbf{f}_l)}{\partial g_{l,i}}, \tag{78}$$

$$\frac{\partial \mathbf{q}_{\text{NU}}(\mathbf{g}_l, \mathbf{f}_l)}{\partial g_{l,i}} = \frac{\partial \mathbf{a}_{\mathbf{d}_t}^* (\mathbf{g}_l) \otimes \mathbf{b}_{\mathbf{d}_r} (\mathbf{f}_l)}{\partial g_{l,i}} = \frac{\partial \mathbf{a}_{\mathbf{d}_t}^* (\mathbf{g}_l)}{\partial g_{l,i}} \otimes \mathbf{b}_{\mathbf{d}_r} (\mathbf{f}_l), \tag{79}$$

$$\frac{\partial \mathbf{a}_{\mathbf{d}_t}^* (\mathbf{g}_l)}{\partial g_{l,i}} = \left( \frac{-j2\pi}{\lambda} [d_{t,i}(1), \ldots, d_{t,i}(N)]^T \right) \circ \mathbf{a}_{\mathbf{d}_t}^* (\mathbf{g}_l). \tag{80}$$

By plugging (80) into (77), we have (71). Similarly we can obtain (72).

## B. Derivation for (73)

The gradient with respect to $\sigma_l$ can be calculated by

$$
\begin{aligned}
\nabla_{\sigma_l} \Gamma \left( \{ \mathbf{g}_l, \mathbf{f}_l, \sigma_l \} \right) &= \frac{\partial \left( \mu \| \boldsymbol{\sigma} \|_1 + \frac{1}{2} \left\| \mathbf{y} - \bar{\mathbf{P}} \mathbf{h} \right\|_2^2 \right)}{\partial \sigma_l^*} \\
&= \frac{\partial \| \boldsymbol{\sigma} \|_1}{\partial \sigma_l^*} - \frac{1}{2} \frac{\partial \mathbf{y}^H \bar{\mathbf{P}} \mathbf{h}}{\partial \sigma_l^*} - \frac{1}{2} \frac{\partial \mathbf{h}^H \bar{\mathbf{P}}^H \mathbf{y}}{\partial \sigma_l^*} + \frac{1}{2} \frac{\partial \mathbf{h}^H \bar{\mathbf{P}}^H \bar{\mathbf{P}} \mathbf{h}}{\partial \sigma_l^*},
\end{aligned} \tag{81}
$$

where

$$\frac{\partial \mathbf{y}^H \bar{\mathbf{P}} \mathbf{h}}{\partial \sigma_l^*} = \mathbf{y}^H \bar{\mathbf{P}} \mathbf{q}_{\text{NU}} (\mathbf{g}_l, \mathbf{f}_l) \frac{\partial \sigma_l}{\partial \sigma_l^*} = 0, \tag{82}$$

$$\frac{\partial \mathbf{h}^H \bar{\mathbf{P}}^H \mathbf{y}}{\partial \sigma_l^*} = \left( \left( \bar{\mathbf{P}} \mathbf{q}_{\text{NU}} (\mathbf{g}_l, \mathbf{f}_l) \right)^H \mathbf{y} \right)^T \frac{\partial \sigma_l^*}{\partial \sigma_l^*} = \left( \left( \bar{\mathbf{P}} \mathbf{q}_{\text{NU}} (\mathbf{g}_l, \mathbf{f}_l) \right)^H \mathbf{y} \right)^T, \tag{83}$$

$$\frac{\partial \mathbf{h}^H \bar{\mathbf{P}}^H \bar{\mathbf{P}} \mathbf{h}}{\partial \sigma_l^*} = \left( \left( \bar{\mathbf{P}} \mathbf{q}_{\text{NU}} (\mathbf{g}, \mathbf{f}) \right)^H \bar{\mathbf{P}} \mathbf{q}_{\text{NU}} (\mathbf{g}_l, \mathbf{f}_l) \sigma_l \right)^T, \tag{84}$$

$$
\begin{aligned}
\frac{\partial \| \boldsymbol{\sigma} \|_1}{\partial \sigma_l^*} &= \frac{\partial \sum_l |\sigma_l|}{\partial \sigma_l^*} = \frac{\partial |\sigma_l|}{\partial \sigma_l^*} = \frac{1}{2} \left( \frac{\partial |\sigma_l|}{\partial \mathcal{R}\{\sigma_l\}} + i \frac{\partial |\sigma_l|}{\partial \mathcal{I}\{\sigma_l\}} \right) \\
&= \frac{1}{2} \left( \frac{\partial \sqrt{\mathcal{R}^2\{\sigma_l\} + \mathcal{I}^2\{\sigma_l\}}}{\partial \mathcal{R}\{\sigma_l\}} + i \frac{\partial \sqrt{\mathcal{R}^2\{\sigma_l\} + \mathcal{I}^2\{\sigma_l\}}}{\partial \mathcal{I}\{\sigma_l\}} \right) \\
&= \frac{\sigma_l}{2|\sigma_l|},
\end{aligned} \tag{85}
$$

where $\mathcal{I}\{\cdot\}$ returns the imaginary part of the input. Plugging (82)-(85) into (81), we obtain (73).

## REFERENCES

[1] T. S. Rappaport, S. Sun, R. Mayzus, H. Zhao, Y. Azar, K. Wang, G. N. Wong, J. K. Schulz, M. Samimi, and F. Gutierrez, "Millimeter wave mobile communications for 5g cellular: It will work!" *IEEE Access*, vol. 1, pp. 335–349, 2013.

[2] X. Cheng, B. Yu, L. Yang, J. Zhang, G. Liu, Y. Wu, and L. Wan, "Communicating in the real world: 3d mimo," *IEEE Wireless Communications*, vol. 21, no. 4, pp. 136–144, August 2014.

[3] S. Hur, T. Kim, D. J. Love, J. V. Krogmeier, T. A. Thomas, and A. Ghosh, "Millimeter wave beamforming for wireless backhaul and access in small cell networks," *IEEE Trans. Commun.*, vol. 61, no. 10, pp. 4391–4403, October 2013.

[4] Y. H. Nam, B. L. Ng, K. Sayana, Y. Li, J. Zhang, Y. Kim, and J. Lee, "Full-dimension mimo (fd-mimo) for next generation cellular technology," *IEEE Communications Magazine*, vol. 51, no. 6, pp. 172–179, June 2013.

[5] S. Kutty and D. Sen, "Beamforming for millimeter wave communications: An inclusive survey," *IEEE Communications Surveys Tutorials*, vol. 18, no. 2, pp. 949–973, Secondquarter 2016.

[6] J. Wang, "Beam codebook based beamforming protocol for multi-gbps millimeter-wave wpan systems," *IEEE Journal on Selected Areas in Communications*, vol. 27, no. 8, pp. 1390–1399, October 2009.

[7] M. K. Samimi and T. S. Rappaport, "3-d millimeter-wave statistical channel model for 5g wireless system design," *IEEE Transactions on Microwave Theory and Techniques*, vol. 64, no. 7, pp. 2207–2225, July 2016.

[8] T. A. Thomas, H. C. Nguyen, G. R. MacCartney, and T. S. Rappaport, "3d mmwave channel model proposal," in *2014 IEEE 80th Vehicular Technology Conference (VTC2014-Fall)*, Sept 2014, pp. 1–6.

[9] O. E. Ayach, S. Rajagopal, S. Abu-Surra, Z. Pi, and R. W. Heath, "Spatially sparse precoding in millimeter wave mimo systems," *IEEE Trans. Wireless Commun.*, vol. 13, no. 3, pp. 1499–1513, March 2014.

[10] A. Alkhateeb, O. E. Ayach, G. Leus, and R. W. Heath, "Channel estimation and hybrid precoding for millimeter wave cellular systems," *IEEE Journal of Selected Topics in Signal Processing*, vol. 8, no. 5, pp. 831–846, Oct 2014.

[11] A. Alkhateeby, G. Leusz, and R. W. Heath, "Compressed sensing based multi-user millimeter wave systems: How many measurements are needed?" in *2015 IEEE International Conference on Acoustics, Speech and Signal Processing (ICASSP)*, April 2015, pp. 2909–2913.

[12] Z. Guo, X. Wang, and W. Heng, "Millimeter-wave channel estimation based on two-dimensional beamspace music method," *IEEE Transactions on Wireless Communications*, vol. PP, no. 99, 2017.

[13] S. Sun and T. S. Rappaport, "Millimeter wave mimo channel estimation based on adaptive compressed sensing," in *2017 IEEE International Conference on Communications Workshops (ICC Workshops)*, May 2017, pp. 47–53.

[14] D. L. Donoho, "Compressed sensing," *IEEE Trans. Inform. Theory*, vol. 52, no. 4, pp. 1289–1306, April 2006.

[15] T. S. Rappaport, R. W. Heath, R. C. Daniels, and J. N. Murdock, *Millimeter Wave Wireless Communication*. Prentice-Hall, 2014.

[16] G. Tang, B. N. Bhaskar, P. Shah, and B. Recht, "Compressed sensing off the grid," *IEEE Trans. Inform. Theory*, vol. 59, no. 11, pp. 7465–7490, Nov 2013.

[17] B. N. Bhaskar, G. Tang, and B. Recht, "Atomic norm denoising with applications to line spectral estimation," *IEEE Trans. Sig. Proc.*, vol. 61, no. 23, pp. 5987–5999, 2013.

[18] J. Steinwandt, F. Roemer, C. Steffens, M. Haardt, and M. Pesavento, "Gridless super-resolution direction finding for strictly non-circular sources based on atomic norm minimization," in *2016 50th Asilomar Conference on Signals, Systems and Computers*, Nov 2016, pp. 1518–1522.

[19] B. N. Bhaskar, G. Tang, and B. Recht, "Atomic norm denoising with applications to line spectral estimation," *IEEE Trans. Sig. Proc.*, vol. 61, no. 23, pp. 5987–5999, Dec 2013.

[20] Y. Zhang, G. Zhang, and X. Wang, "Array covariance matrix-based atomic norm minimization for off-grid coherent direction-of-arrival estimation," in *2017 IEEE International Conference on Acoustics, Speech and Signal Processing (ICASSP)*, March 2017, pp. 3196–3200.

[21] Z. Tian, Z. Zhang, and Y. Wang, "Low-complexity optimization for two-dimensional direction-of-arrival estimation via decoupled atomic norm minimization," in *2017 IEEE International Conference on Acoustics, Speech and Signal Processing (ICASSP)*, March 2017, pp. 3071–3075.

[22] P. Zhang, L. Gan, S. Sun, and C. Ling, "Atomic norm denoising-based channel estimation for massive multiuser mimo systems," in *2015 IEEE International Conference on Communications (ICC)*, June 2015, pp. 4564–4569.

[23] P. Shah, B. N. Bhaskar, G. Tang, and B. Recht, "Linear system identification via atomic norm regularization," in *2012 IEEE 51st IEEE Conference on Decision and Control (CDC)*, Dec 2012, pp. 6265–6270.

[24] W. Liu, Z. Wang, C. Sun, S. Chen, and L. Hanzo, "Structured non-uniformly spaced rectangular antenna array design for fd-mimo systems," *IEEE Trans. Wireless Commun.*, vol. 16, no. 5, pp. 3252–3266, May 2017.

[25] P. Wang, Y. Li, Y. Peng, S. C. Liew, and B. Vucetic, "Non-uniform linear antenna array design and optimization for millimeter-wave communications," *IEEE Transactions on Wireless Communications*, vol. 15, no. 11, pp. 7343–7356, Nov 2016.

[26] J. Choi, K. Lee, D. J. Love, T. Kim, and R. W. Heath, "Advanced limited feedback designs for fd-mimo using uniform planar arrays," in *2015 IEEE Global Communications Conference (GLOBECOM)*, Dec 2015, pp. 1–6.

[27] Y. Han, S. Jin, X. Li, Y. Huang, L. Jiang, and G. Wang, "Design of double codebook based on 3d dual-polarized channel for multiuser mimo system," *EURASIP Journal on Advances in Signal Processing*, vol. 2014, no. 1, p. 111, 2014.

[28] D. Yang, L. L. Yang, and L. Hanzo, "Dft-based beamforming weight-vector codebook design for spatially correlated channels in the unitary precoding aided multiuser downlink," in *2010 IEEE International Conference on Communications*, May 2010, pp. 1–5.

[29] J. Lee, G. T. Gil, and Y. H. Lee, "Exploiting spatial sparsity for estimating channels of hybrid mimo systems in millimeter wave communications," in *2014 IEEE Global Communications Conference*, Dec 2014, pp. 3326–3331.

[30] P. Gupta and S. P. Kar, "Music and improved music algorithm to estimate direction of arrival," in *2015 International Conference on Communications and Signal Processing (ICCSP)*, April 2015, pp. 0757–0761.

[31] W. Zhang, W. Liu, J. Wang, and S. Wu, "Joint transmission and reception diversity smoothing for direction finding of coherent targets in mimo radar," *IEEE Journal of Selected Topics in Signal Processing*, vol. 8, no. 1, pp. 115–124, Feb 2014.

[32] Z. Yang and L. Xie, "Exact joint sparse frequency recovery via optimization methods," *IEEE Trans. Sig. Proc.*, vol. 64, no. 19, pp. 5145–5157, Oct 2016.

[33] Z. Yang, L. Xie, and P. Stoica, "Vandermonde decomposition of multilevel toeplitz matrices with application to multidimensional super-resolution," *IEEE Trans. Inform. Theory*, vol. 62, no. 6, pp. 3685–3701, June 2016.

[34] Y. Chi and Y. Chen, "Compressive recovery of 2-d off-grid frequencies," in *2013 Asilomar Conference on Signals, Systems and Computers*, Nov 2013, pp. 687–691.

[35] ——, "Compressive two-dimensional harmonic retrieval via atomic norm minimization," *IEEE Trans. Sig. Proc.*, vol. 63, no. 4, pp. 1030–1042, 2015.

[36] E. J. Candès and C. Fernandez-Granda, "Towards a mathematical theory of super-resolution," *Communications on Pure and Applied Mathematics*, vol. 67, no. 6, pp. 906–956, 2014.

[37] L. Zheng and X. Wang, "Super-resolution delay-doppler estimation for ofdm passive radar," *IEEE Trans. Sig. Proc.*, vol. 65, no. 9, pp. 2197–2210, May 2017.

[38] Z. Tian, Z. Zhang, and Y. Wang, "Low-complexity optimization for two-dimensional direction-of-arrival estimation via decoupled atomic norm minimization," in *2017 IEEE International Conference on Acoustics, Speech and Signal Processing (ICASSP)*, March 2017, pp. 3071–3075.

[39] S. Boyd, N. Parikh, E. Chu, B. Peleato, and J. Eckstein, "Distributed optimization and statistical learning via the alternating direction method of multipliers," *Foundations and Trends® in Machine Learning*, vol. 3, no. 1, pp. 1–122, 2011.

[40] J. F. Sturm, "Using sedumi 1.02, a matlab toolbox for optimization over symmetric cones," *Optimization methods and software*, vol. 11, no. 1-4, pp. 625–653, 1999.

[41] K.-C. Toh, M. J. Todd, and R. H. Tutuncu, "Sdpt3-a matlab software package for semidefinite programming, version 1.3," *Optimization methods and software*, vol. 11, no. 1-4, pp. 545–581, 1999.

[42] E. Torkildson, C. Sheldon, U. Madhow, and M. Rodwell, "Nonuniform array design for robust millimeter-wave mimo links," in *GLOBECOM 2009 - 2009 IEEE Global Telecommunications Conference*, Nov 2009, pp. 1–7.

[43] S. E. Nai, W. Ser, Z. L. Yu, and H. Chen, "Beampattern synthesis for linear and planar arrays with antenna selection by convex optimization," *IEEE Transactions on Antennas and Propagation*, vol. 58, no. 12, pp. 3923–3930, 2010.

[44] Q. Li and G. Tang, "Approximate support recovery of atomic line spectral estimation: A tale of resolution and precision," in *Signal and Information Processing (GlobalSIP), 2016 IEEE Global Conference on.* IEEE, 2016, pp. 153–156.

[45] N. Boumal and P.-A. Absil, "Low-rank matrix completion via preconditioned optimization on the grassmann manifold," *Linear Algebra and its Applications*, vol. 475, pp. 200–239, 2015.

[46] T. T. Cai and L. Wang, "Orthogonal matching pursuit for sparse signal recovery with noise," *IEEE Trans. Inform. Theory*, vol. 57, no. 7, pp. 4680–4688, July 2011.

[47] M. Grant and S. Boyd, "CVX: Matlab software for disciplined convex programming, version 2.1," http://cvxr.com/cvx, Mar. 2014.